The Importance of Research on Materials

Nitrides seem to be good for everything

Dilute Nitrides

(Ga,In)(N,P,As)

cubic

Conventional Nitrides

AlN, GaN, InN

hexagonal (cubic)

Ferromagnetic Nitrides

TE- and RE-doped

hexagonal (cubic)

Nitrides seem to be good for everything

Dilute Nitrides

(Ga,In)(N,P,As)

cubic

Conventional Nitrides

AlN, GaN, InN

hexagonal (cubic)

Ferromagnetic Nitrides

TE- and RE-doped

hexagonal (cubic)

Conventional III-Nitrides

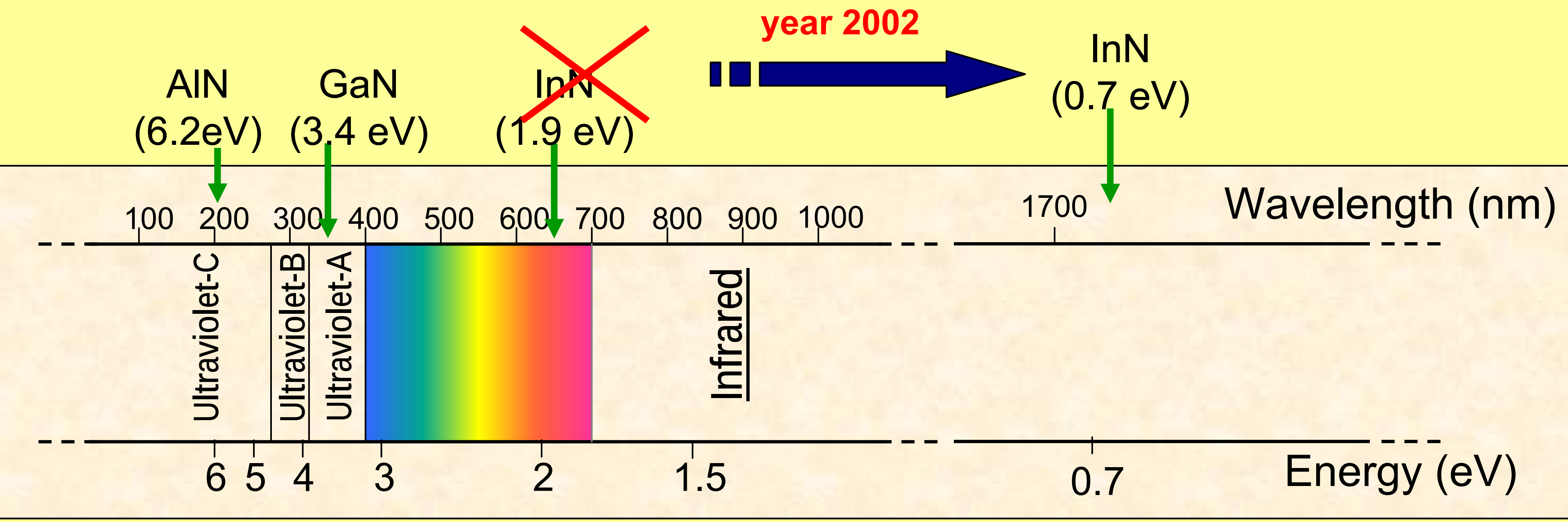

- Direct-gap semiconductors covering wide range 0.7-6.2 eV

    → IR-Blue-UV optical emitters/detectors

- Strong chemical bonding - high stability/resistance

    → high temperature/power electronics

Luminous efficacy of light sources

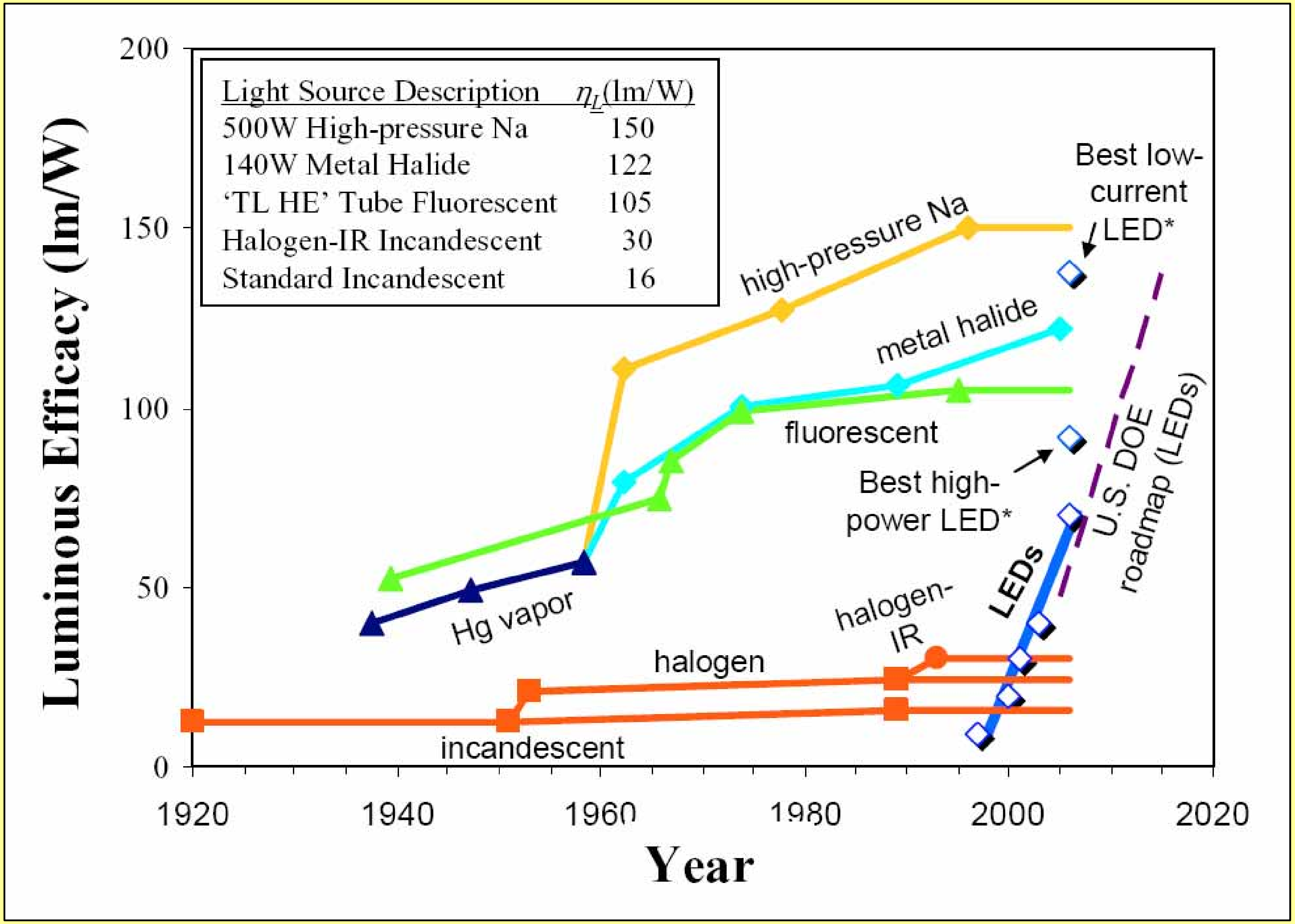

M.G.Craford, OIDA Annual Forum, Washington, Dec.2006.

State-of-Art: High-Power LEDs (1 W)

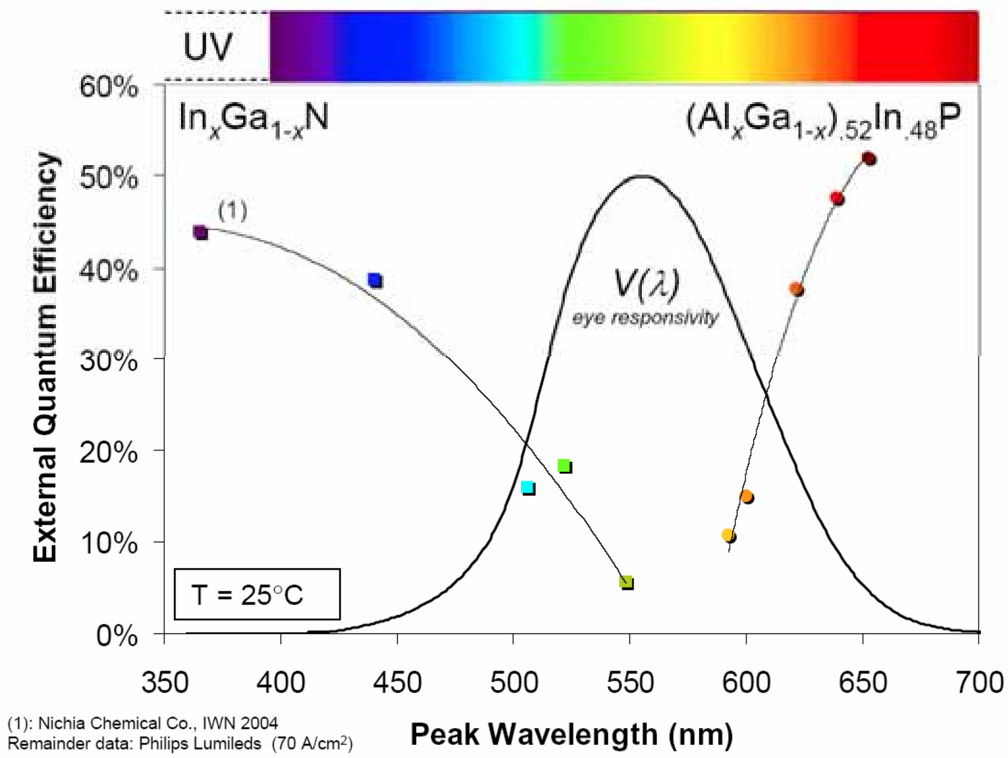

III-P:
- Fundamental band-structure limitations

III-N:
- IQE (~450 nm) ~50 %
- IQE (~520 nm) ~20 %

- External Quantum Efficiency: EQE = Internal QE × Extraction Efficiency
  $EQE = P_{optical} / (E_{ph} \times I_f)$
- Power Conversion/Wallplug Efficiency: PCE or WPE = $P_{optical} / (V_f \times I_f)$
- Luminous Efficacy (lumens/Watt): LE = PCE × V (λ)

M.G.Craford, OIDA Annual Forum, Washington, Dec.2006.

GaN substrate technology

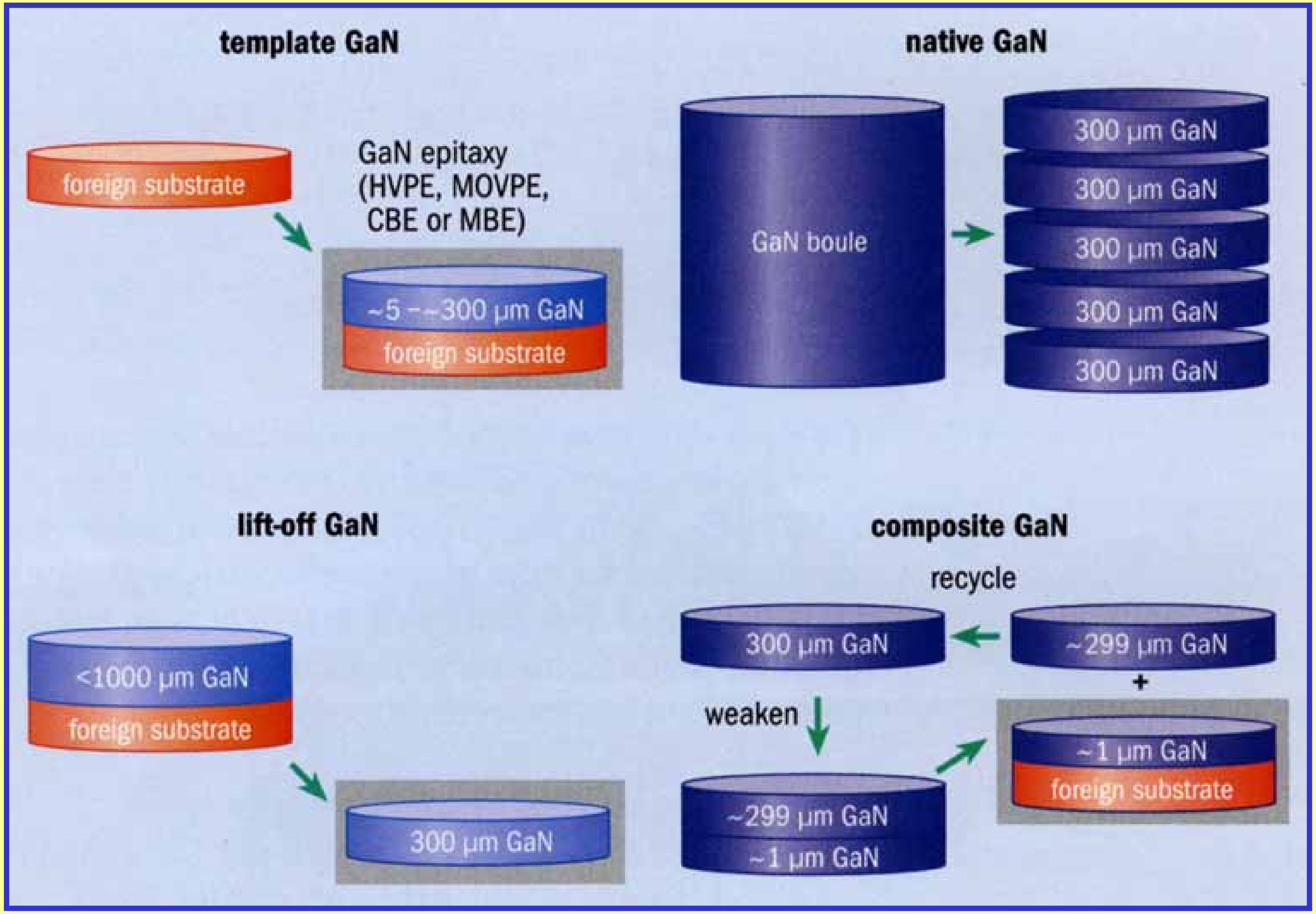

CS August 2007, p.23

Vertical cavity surface emitter (VCSEL)

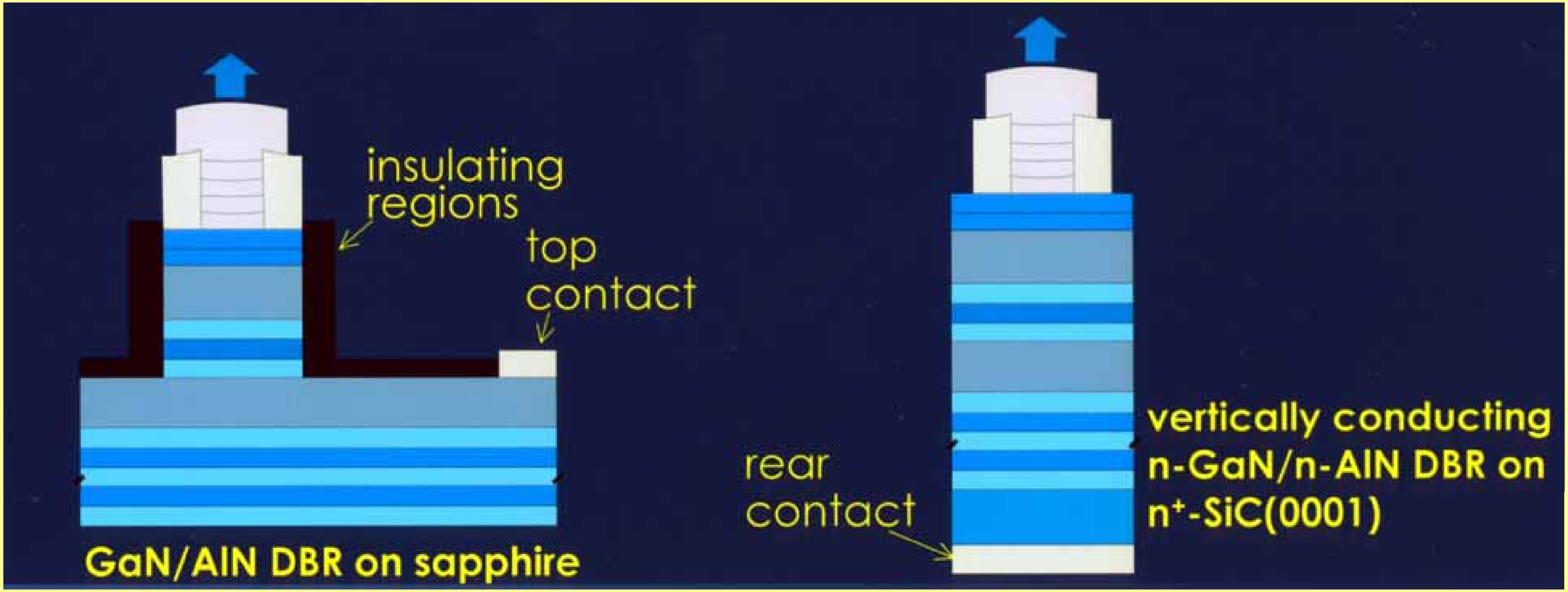

Vertical cavity surface emitter (VCSEL)

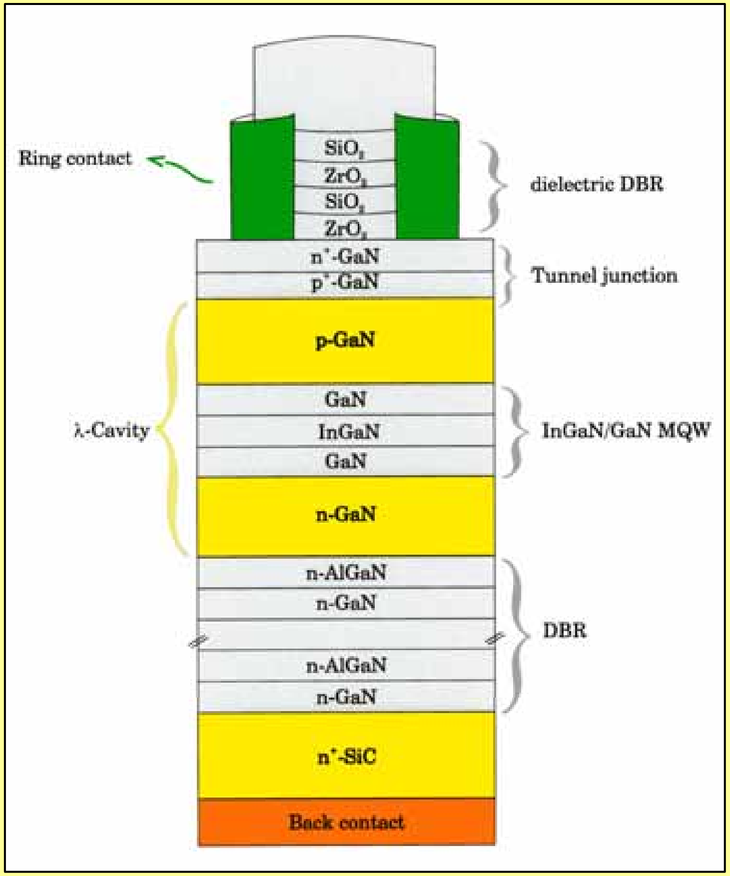

- ➢Improve reflectivity of III-Nitrid Bragg reflector
- ➢Compare strained AlN/GaN DBR with lattice-matched (Al,In)N/GaN DBR
- ➢Reduce series resistance of doped Bragg reflector
- ➢Design and realize p-type carrier injection scheme via tunneling junction

III-Nitride based microcavities to study the formation of exciton polaritons for Bose Einstein condensation

Reflectance of AlN/GaN DBR

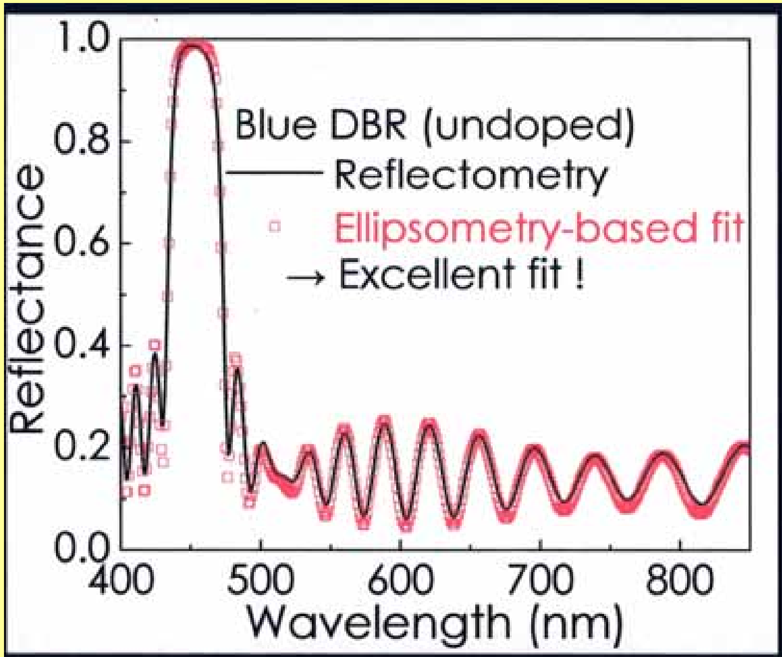

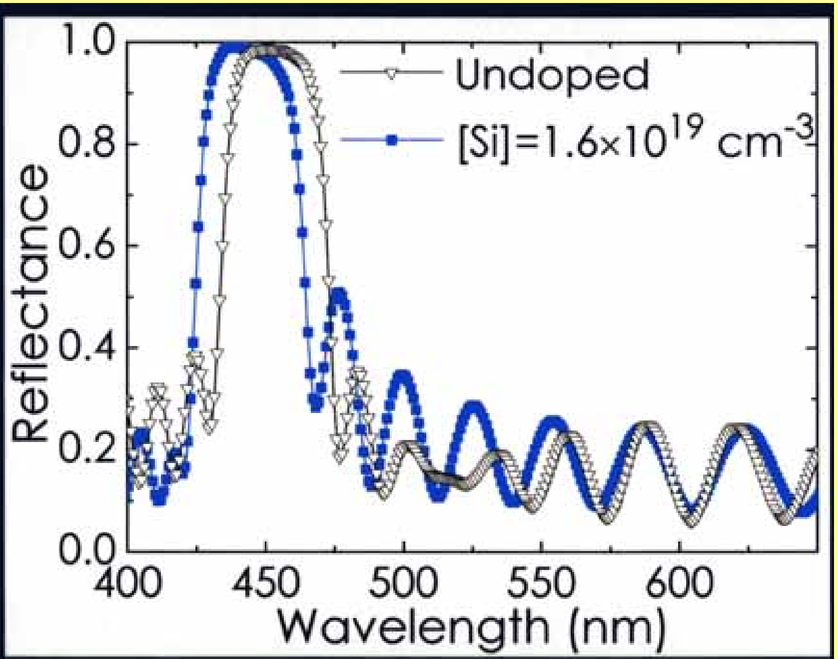

[Si]	R	λ (nm)	FWHW (nm)	d_{AlN} (nm)	d_{GaN} (nm)
Undoped	0.99	454	41	57	46
1.6×10^{19} cm^{-3}	>0.99	445	41	56	45

⇨ Si-doping does not degrade R

GaN electron devices

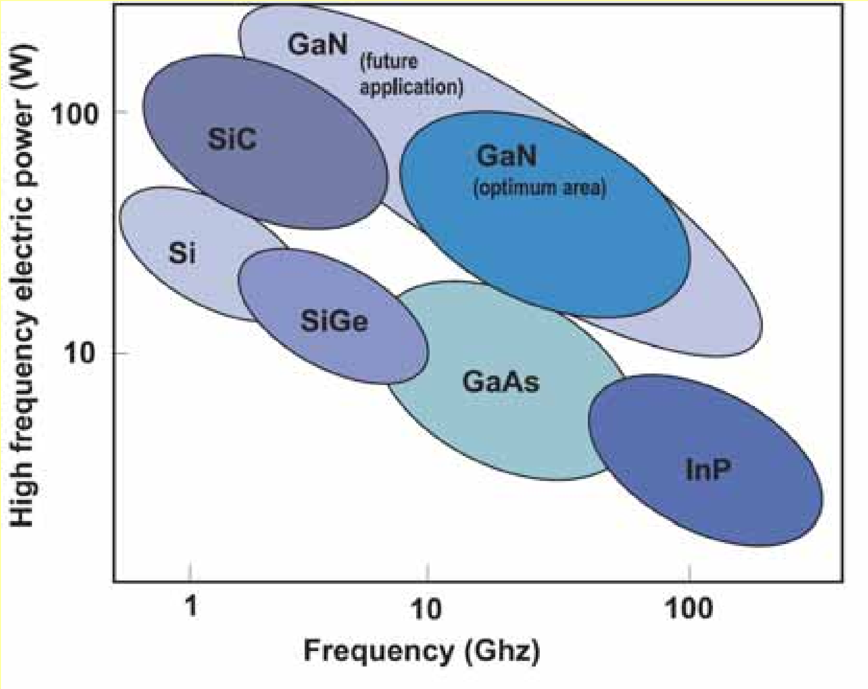

Heterostructure FETs (HFETs, HEMTs)

- **High breakdown electric field**
- **High electron density**
- **High saturation drift velocity**
- **High power output, high frequency and high temperature operation**

Earlier problems:

- **Collapse of drain current**
- **Large gate leakage current**

Compare (Al,Ga)N/GaN with (Al,In)N/GaN

Operation of high-power HFETs in 2 GHz band is satisfactory
Concerns: Reliability, production yield, cost, Issues of substrate material: SiC, Si, AlN

Needs for high frequency operation: High power output, high efficiency, high degree of linearity, low power consumption

Number of publications per year

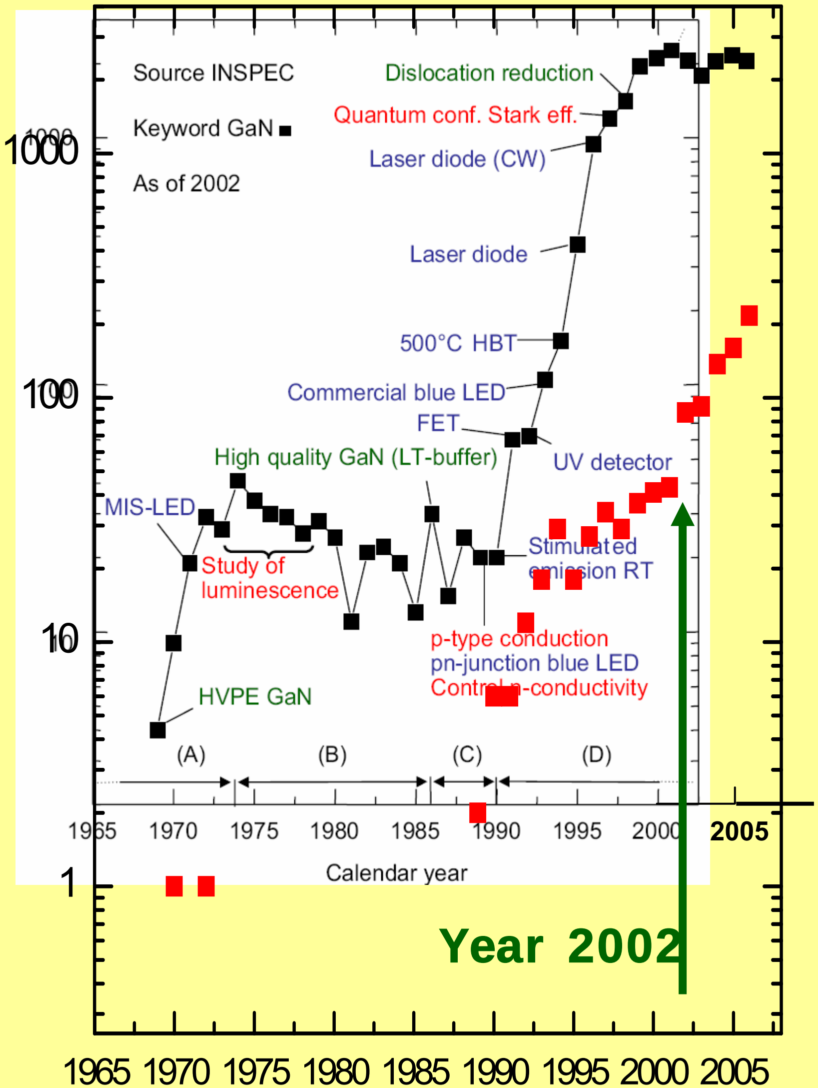

In 2006:

~ **1.800** publications with **GaN** as keyword in title

~ **200** publications with **InN** as keyword in title

Miguel A. Sanchez, EMRS 2007

To do list for InN films

- Improve structural properties of InN films by optimizing growth conditions and proper selection of substrate
- Understand and control the intrinsic electron accumulation on polar InN surfaces
- Grow InN films on nonpolar surfaces

InN nanorods (I)

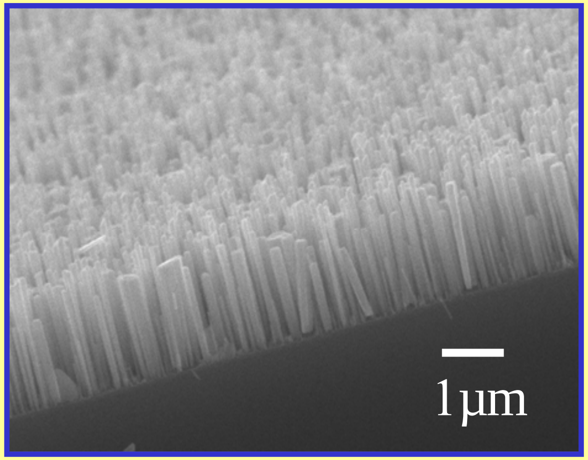

InN/AlN/Si (111)

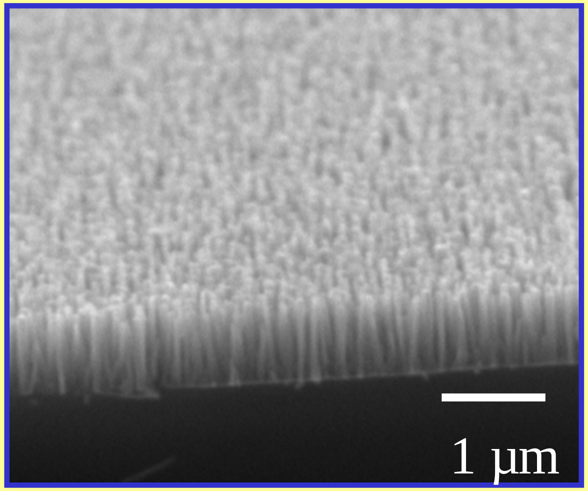

InN /Si (111)

PL Spectra of InN grown with and without buffer layer

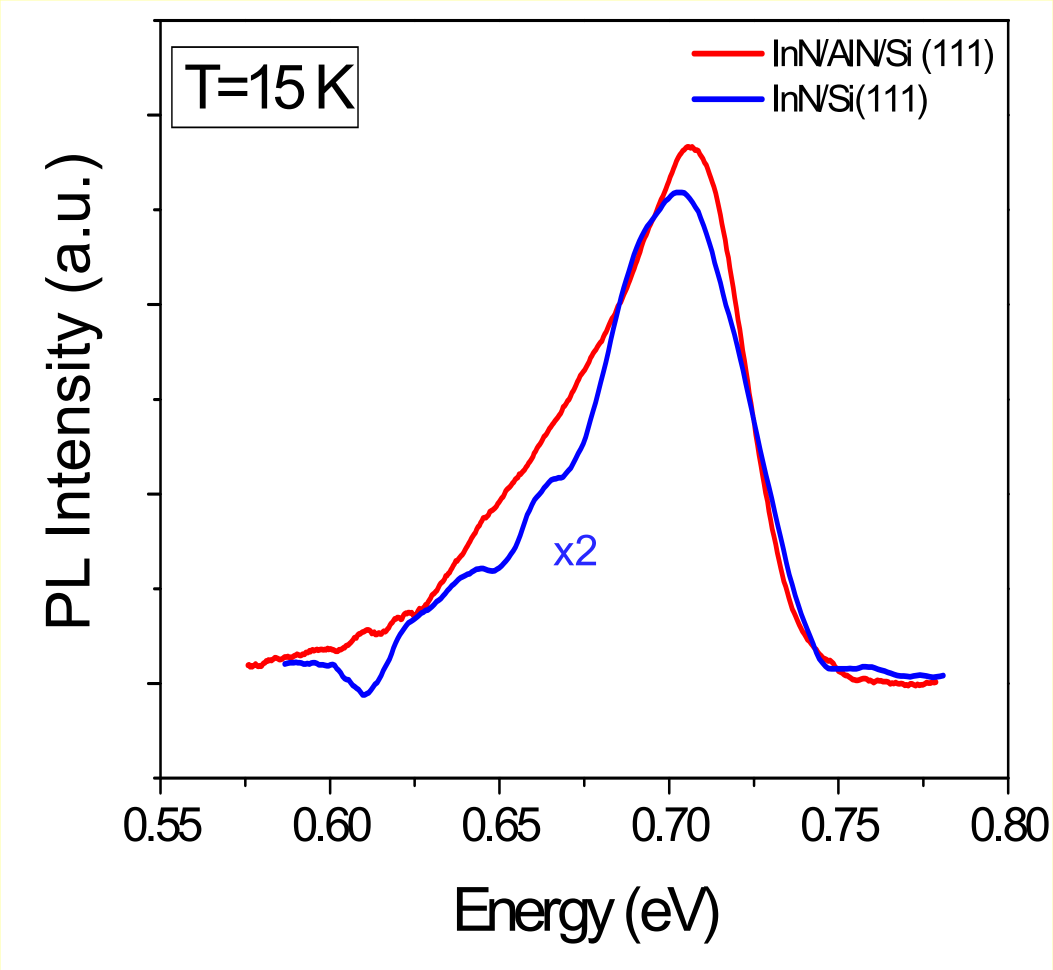

Miguel A. Sanchez, EMRS 2007

InN nanorods (II)

- SEM and TEM photographs of InN nanorods
- SAD pattern reveal epitaxial alignment

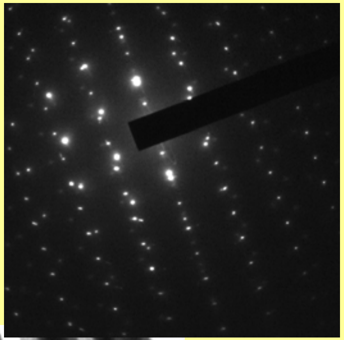

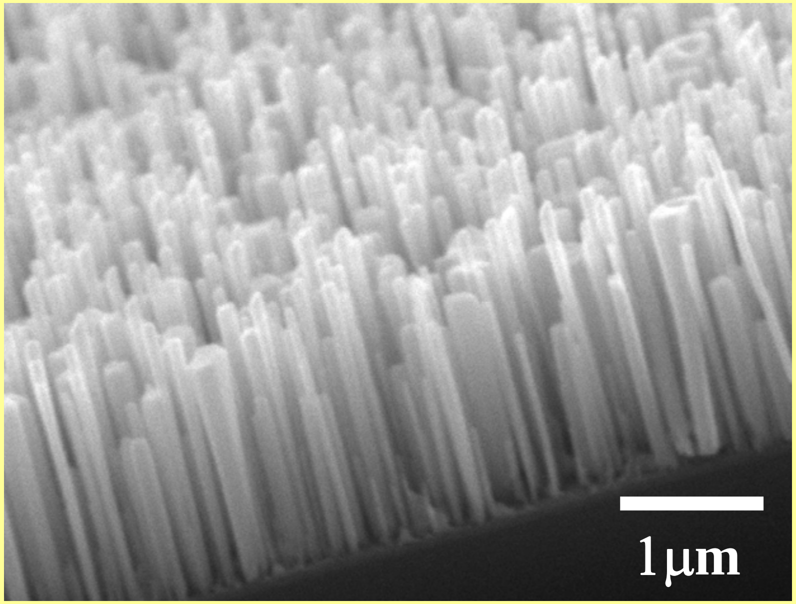

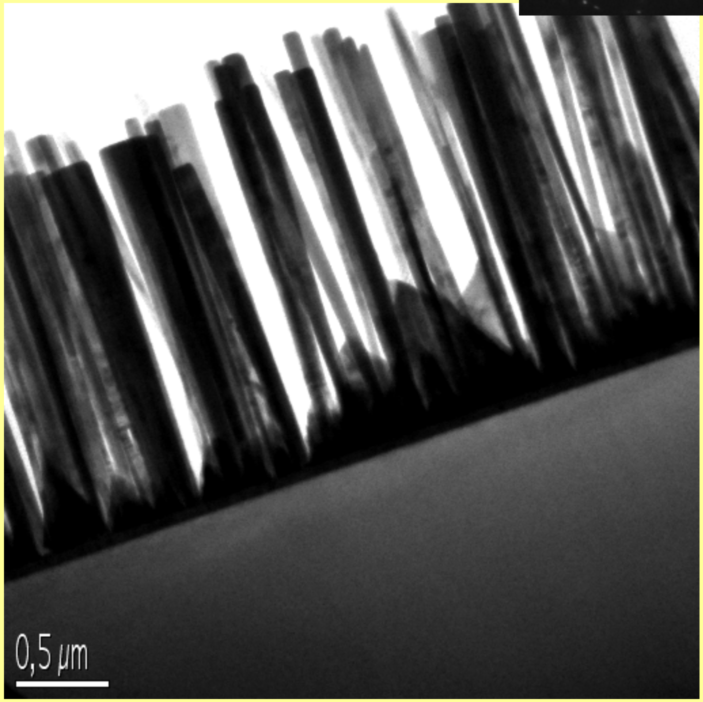

Miguel A. Sanchez, EMRS 2007

InN nanorods (III)

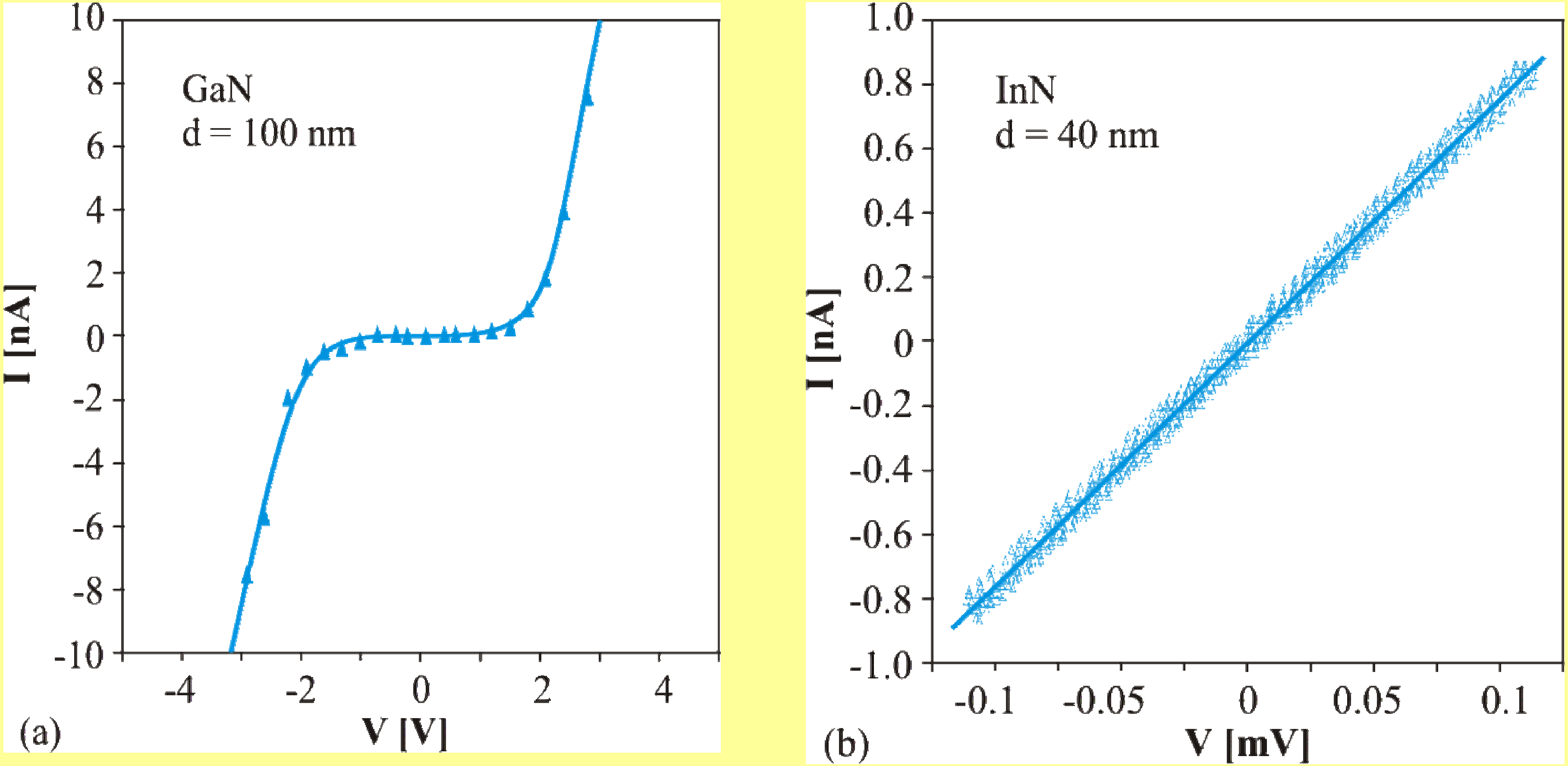

E.Calleja et al. to be published.

Higher conductivity for the InN nanocolumns than for GaN. Related with the tendency of InN to have a very high n-type residual concentration (10^{18} cm^{-3}-$10^{20}$$cm^{-3}$)

Nonpolar GaN

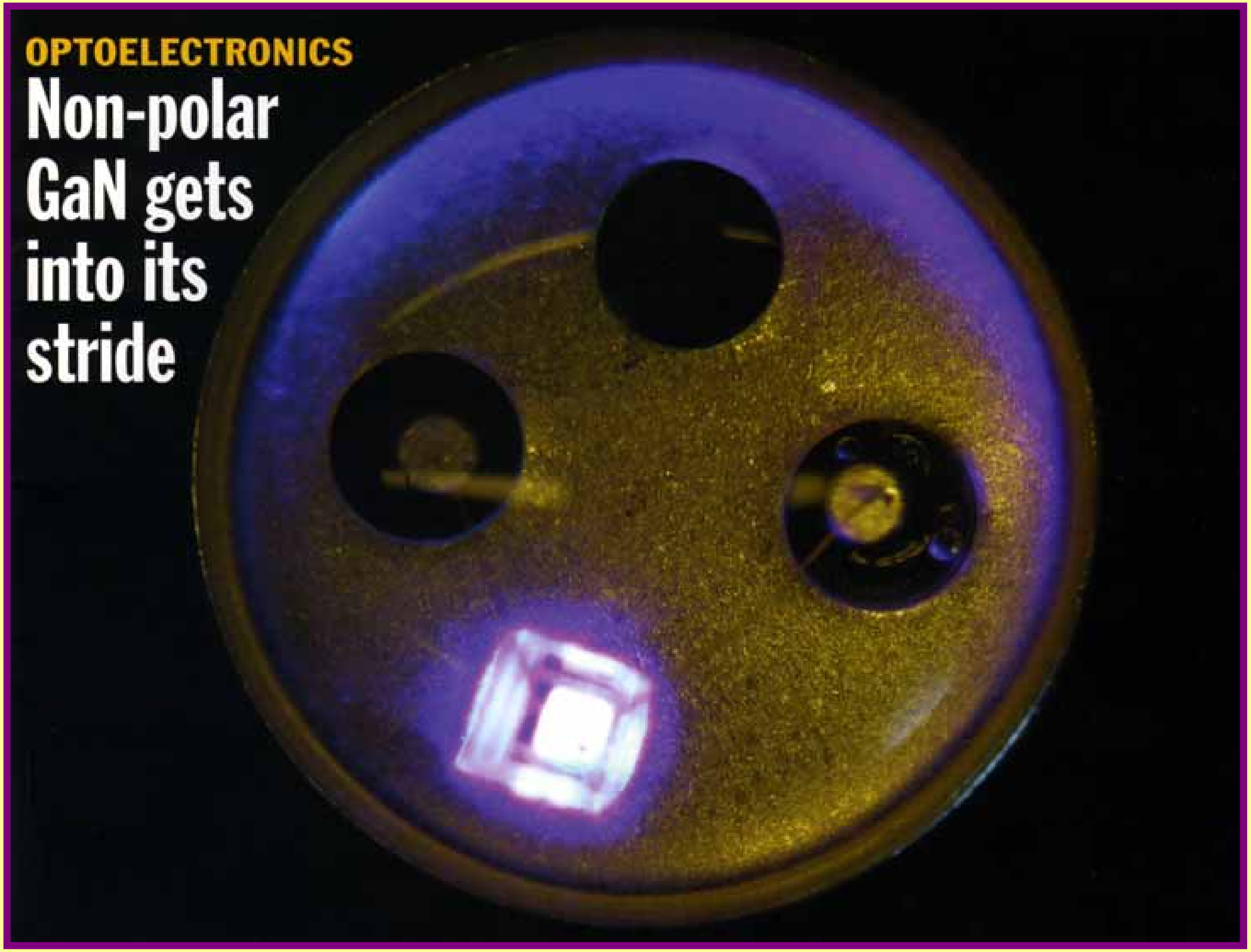

CS June 2007

Origin and consequences of electrical polarization

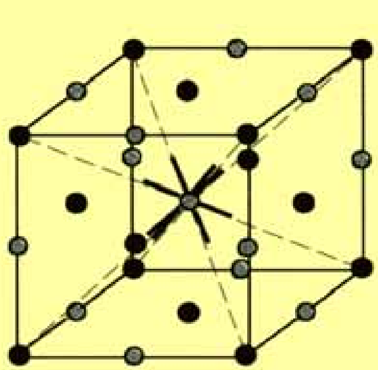

Zincblende GaN

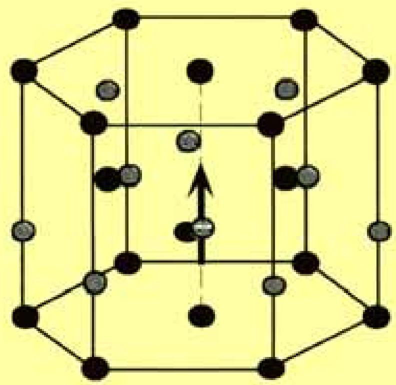

Wurtzite GaN

Zincblende: 4 polar (111) axes
→ piezoelectric along (111)
→ not pyroelectric

Wurtzite: 1 polar (0001) axis
→ piezoelectric along (0001)
→ pyroelectric along (0001)

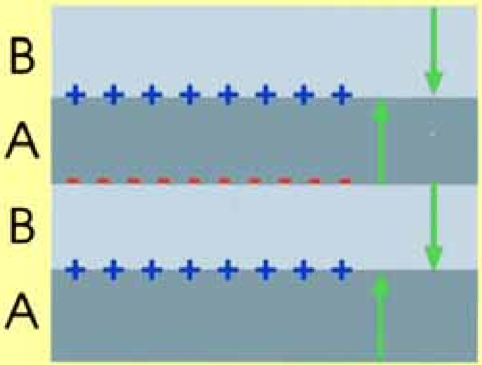

Changes in electrical polarization **along** growth direction

→ Formation of **interface charges**

→ Electric fields along growth direction

Band diagrams of GaN/(Al,Ga)N multiple quantum wells

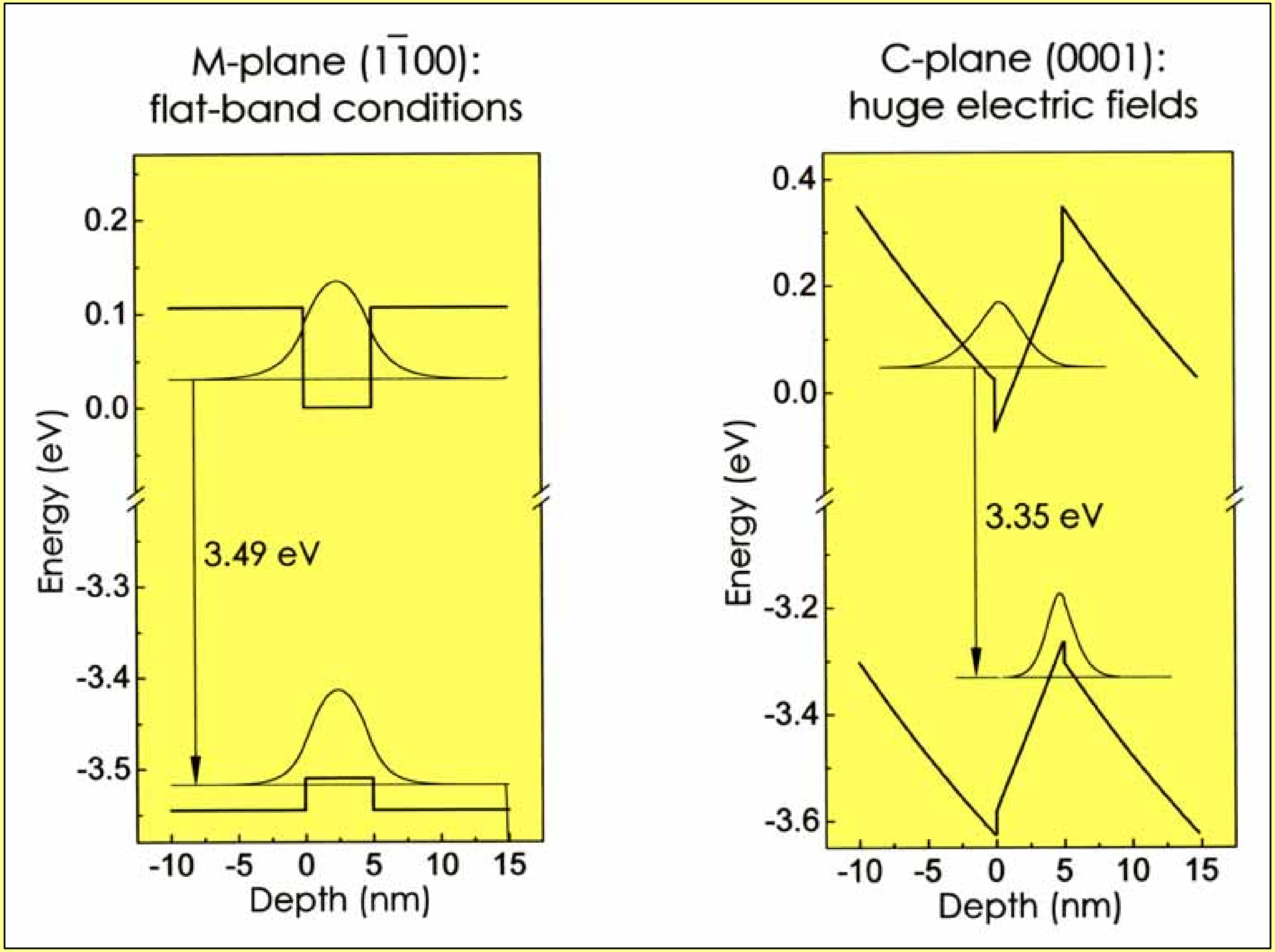

Substrate with small mismatch (γ-$LiAlO_2$) for M-plane GaN

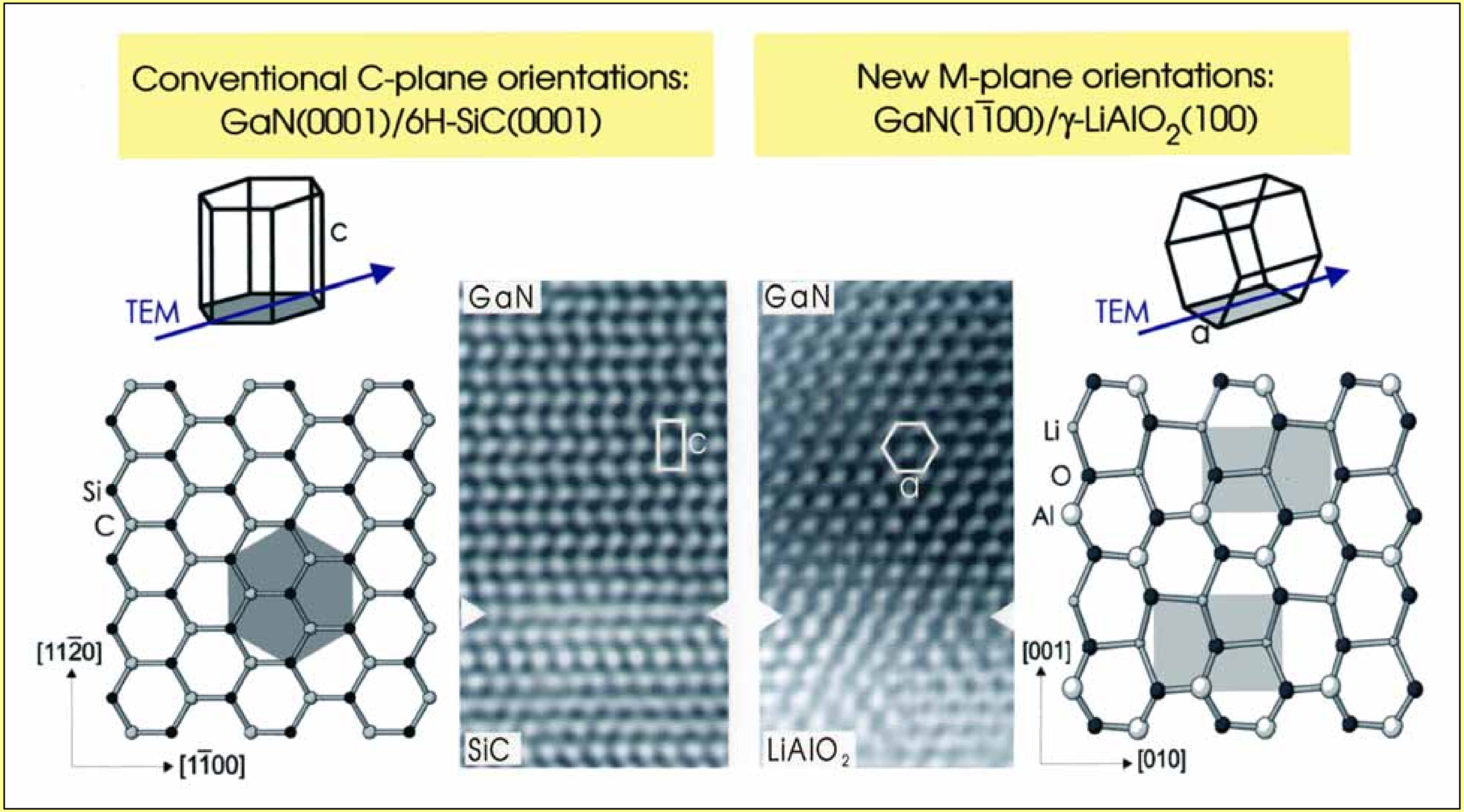

Non-polar GaN

M-plane GaN films grown on γ-$LiAlO_2$

$\rightarrow$ no internal electrostatic fields in QWs
$\rightarrow$ highly anisotropic strain
$\rightarrow$ enhanced optical anisotropy (refractive index, polarization)

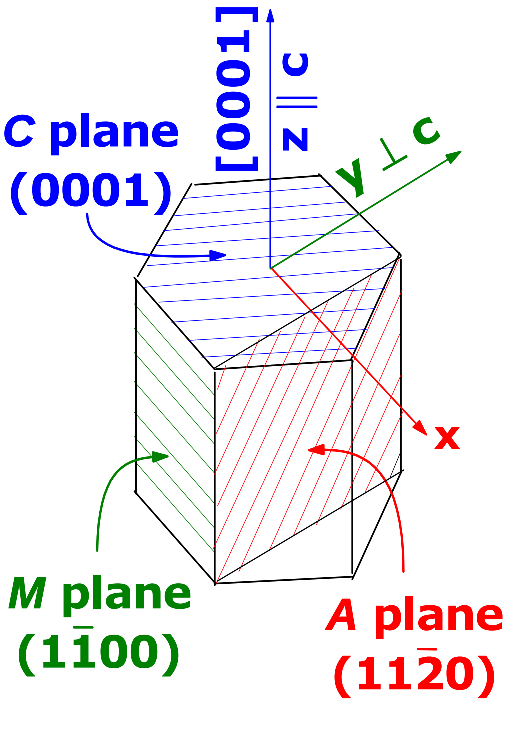

Here:

- linear dichroism
- polarization filtering
- ➢ demonstration of polarization-sensitive photodetectors
- ➢ two-color Bragg reflector (DBR) based on linear birefringence

M-plane GaN photodetectors

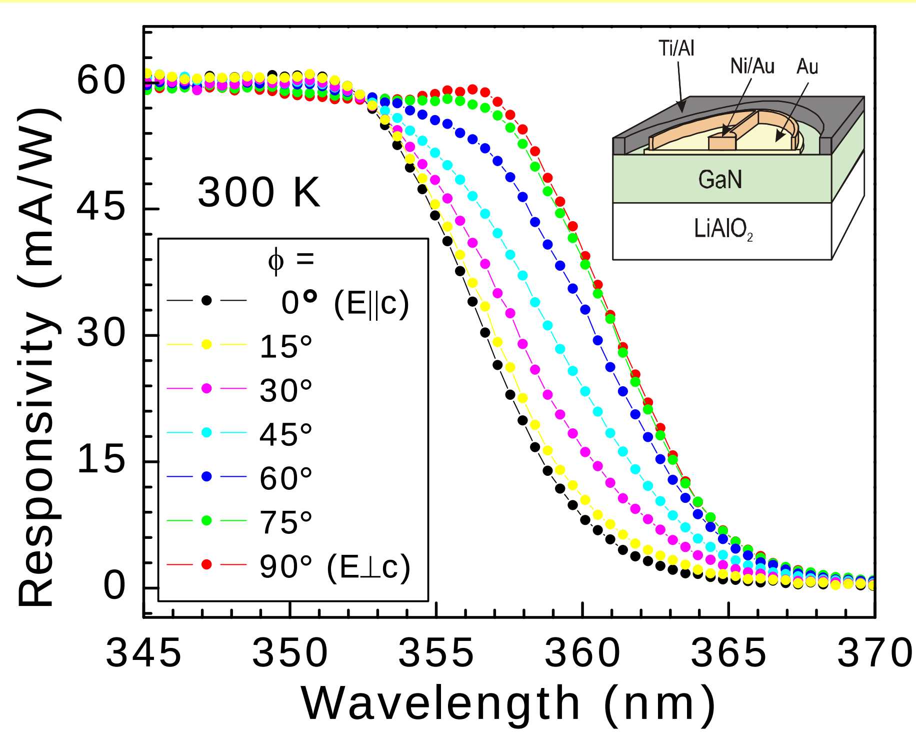

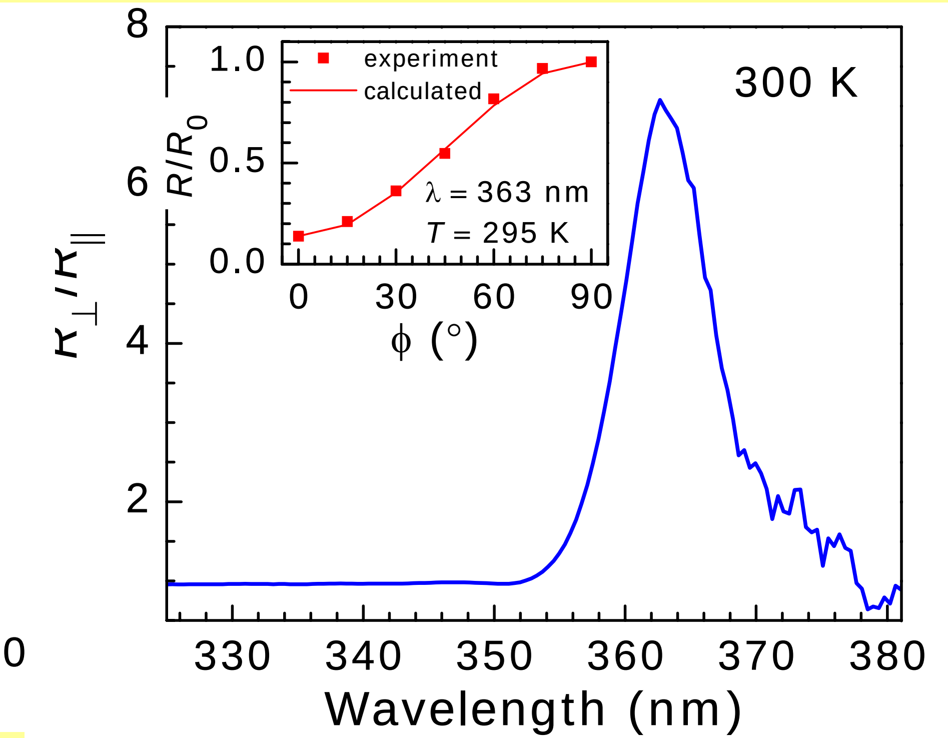

- Photocurrent measurements for semitransparent Schottky diodes, maximum responsivity R=60 mA/W

- Maximum contrast in responsivity >7 at 363 nm

- $R=R_{||}\cos^2\Phi+R_{\wedge}\sin^2\Phi$

H.T Grahn et al

Linear birefringence: two-color M-plane DBR

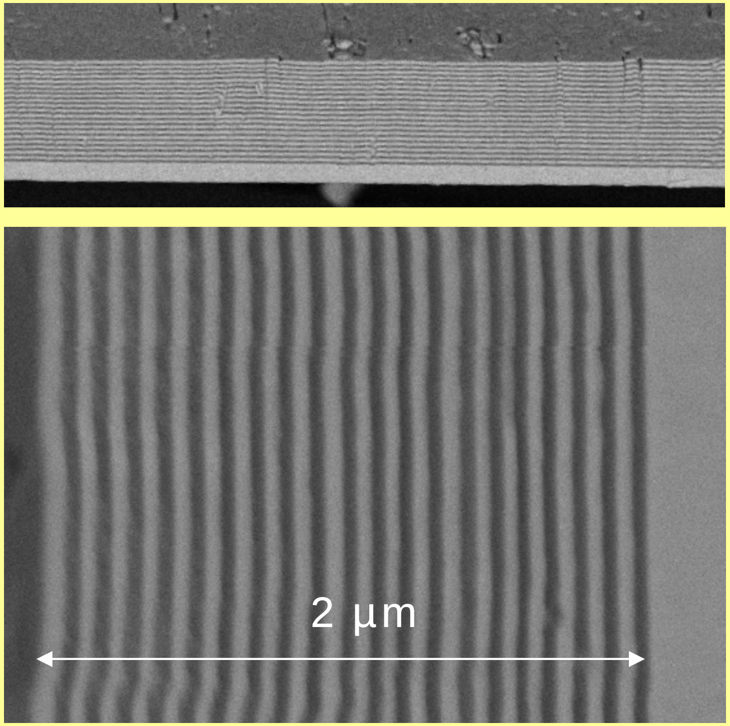

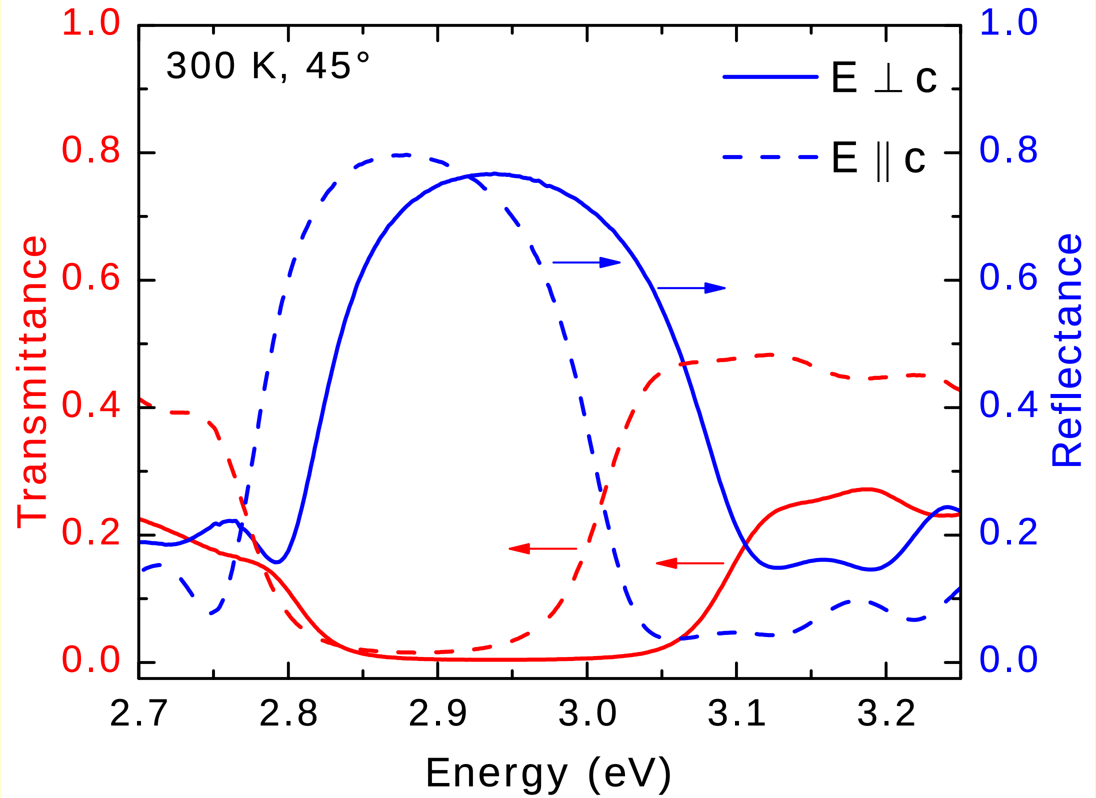

- 20-period GaN/AlN Bragg reflector on ~300 nm GaN buffer layer on $LiAlO_2$
- maximum reflectivity 80–90% limited by interface roughness
- stopband shifts by about 70 meV due to linear birefringence
- maximum contrast between parallel and perpendicular polarization at 3.05 eV

D.M.Schaadt, APL 90(2007)231117

High frequency SAW devices

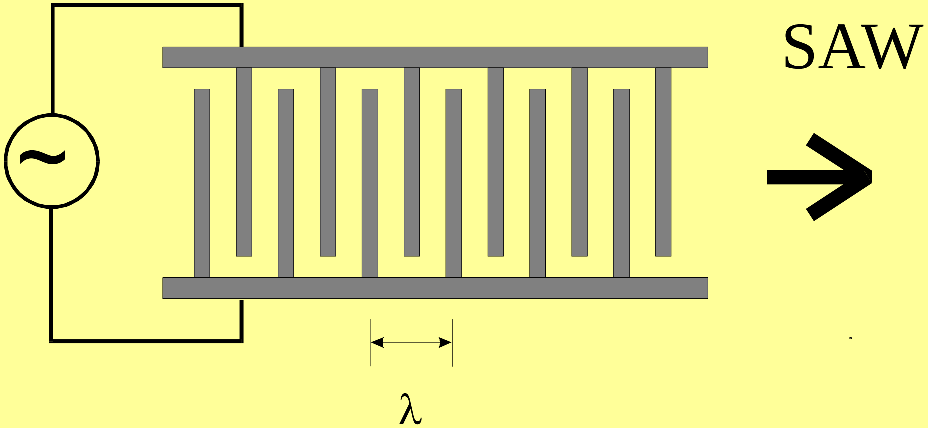

$f = v/\lambda$

For high frequency (f),

small wavelength (λ)

or large velocity (v)

	AlN	GaN	GaAs	$LiNbO_3$
SAW velocity (m/s)	5790	3690	2870	3490-3890
Electromechanical coupling coefficient (%)	0.25	0.13	0.064	4.8

AlN/SiC acoustic heterostructures

AlN is typically grown on substrates such as sapphire, SiC, and Si.

For acoustic applications,
What are the influences of velocity mismatch?

Confinement of acoustic waves in the slow-velocity overlayer.

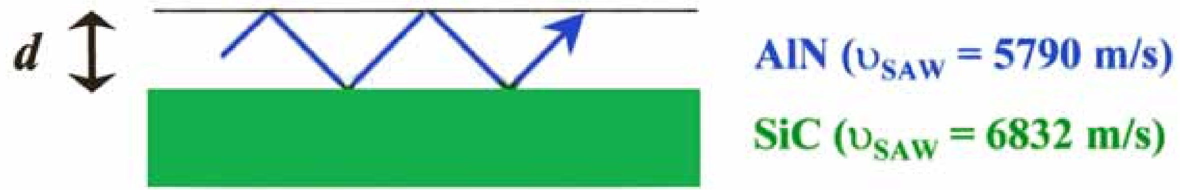

Reflection from the high-velocity substrate (cf. Snell's law).

SAW transmission is mediated by guided modes.

[The guiding is absent if the AlN layer is grown on sapphire or Si because υ_{SAW}(substrate) < υ_{SAW}(AlN).]

Superhigh frequency operation

Our strategy: Electron-beam lithography to reduce λ_{IDT}.
AlN/SiC heterostructures for large υ_{SAW}.

Al (30 nm thick) electrodes

[11$\bar{2}$0]

[1$\bar{1}$00]

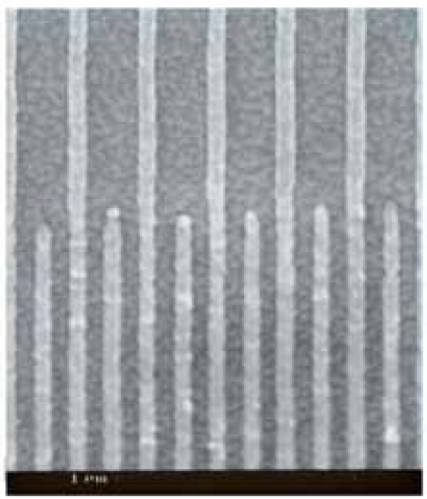

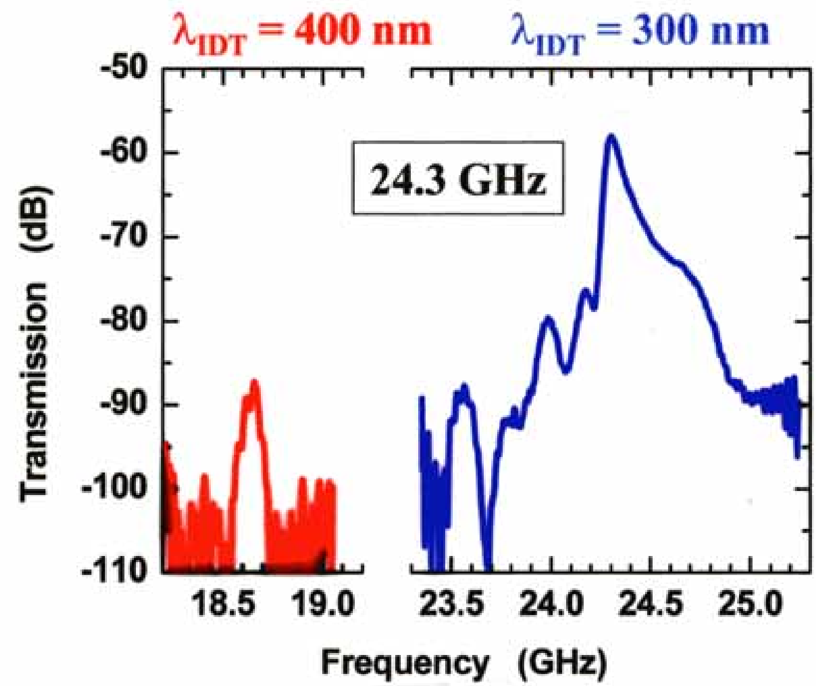

MBE-grown AlN (250 nm thick) layer on 4H-SiC(0001).

SAW propagation is isotropic in the C-plane of hexagonal crystals.

Transmission characteristics

Al electrodes on AlN/SiC

(λ = 400 nm)

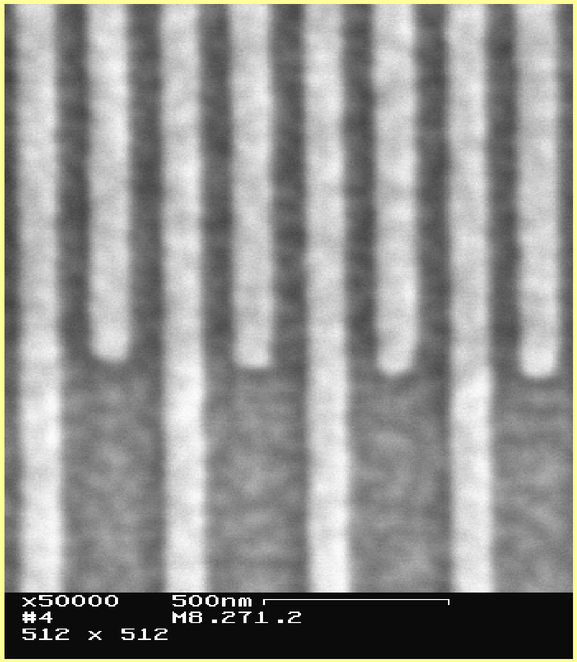

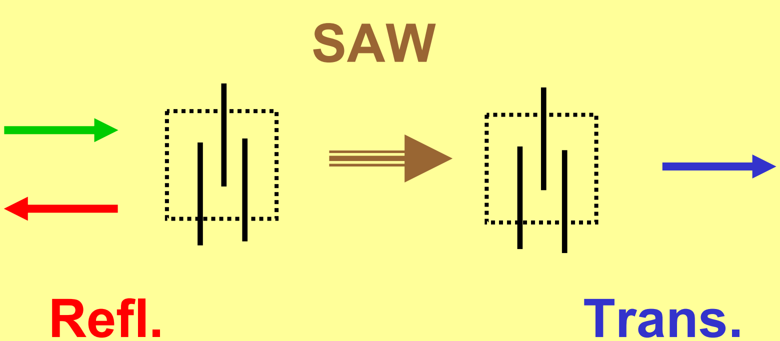

λ = 700 nm, d = 1.25 mm

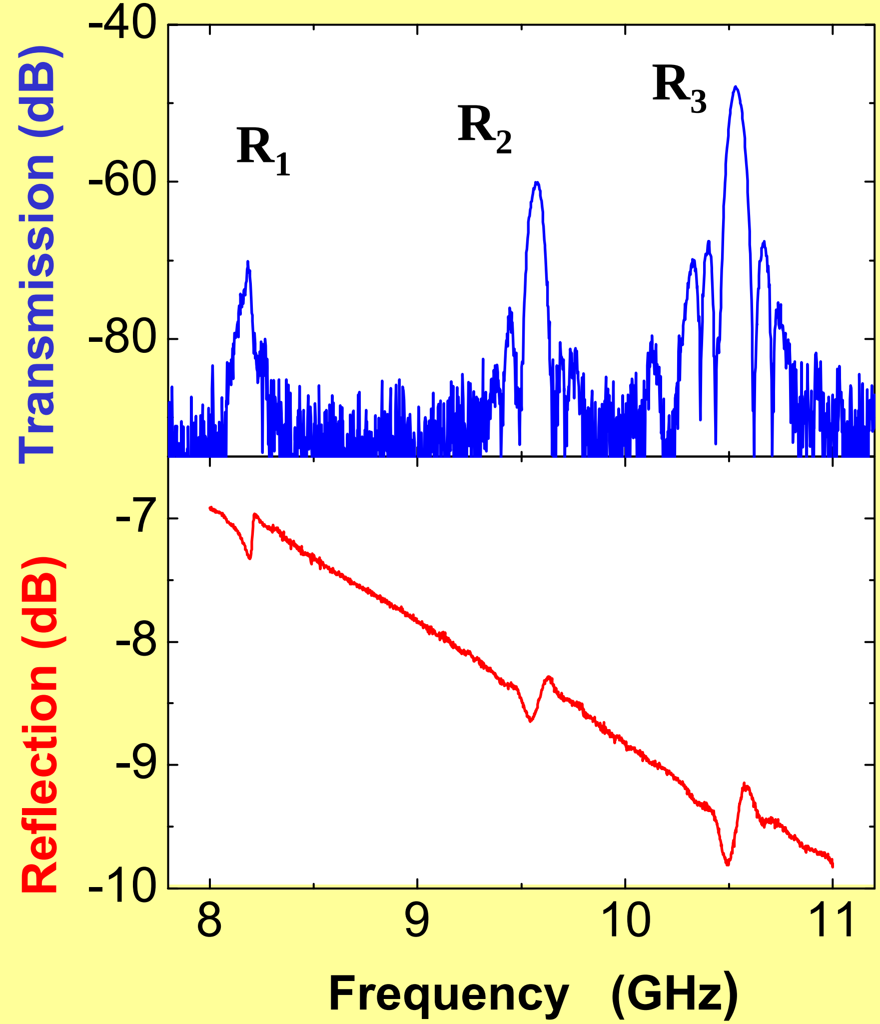

SAW dispersion (hard-supported layer)

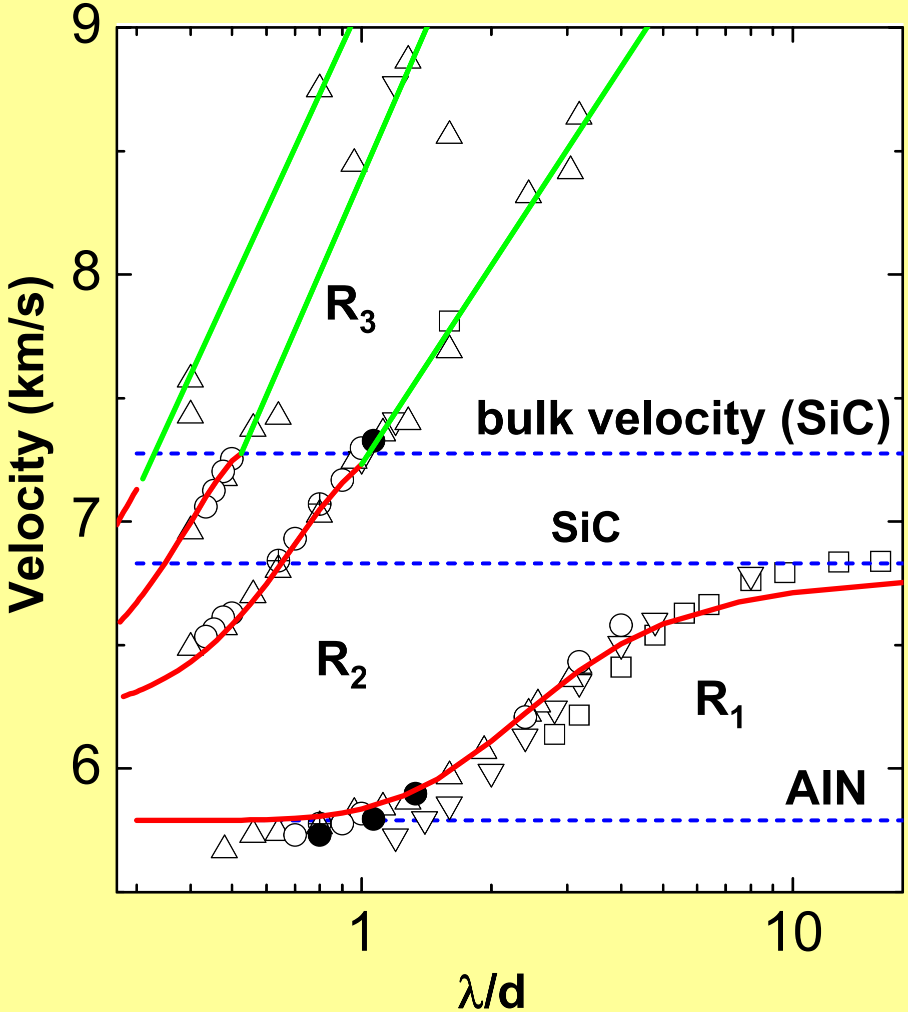

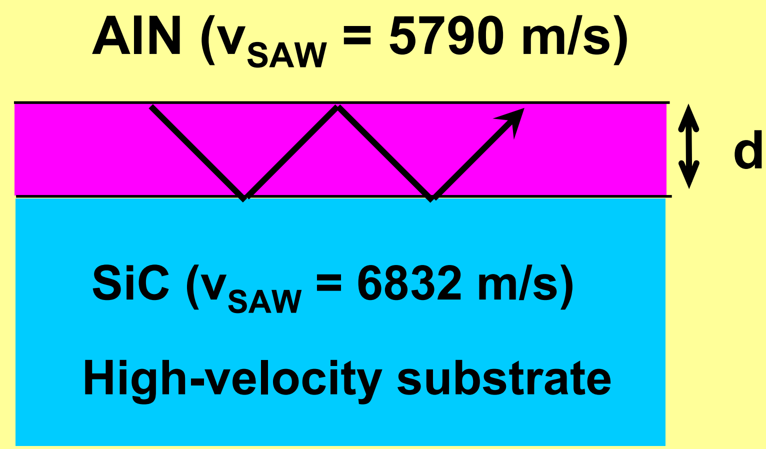

Confinement of acoustic wave in low-velocity layer

(“Quantized” modes in acoustic well)

AlN/GaN/g-LiAlO2 for MEMS/NEMS

// [0001] // [$11\bar{2}0$]

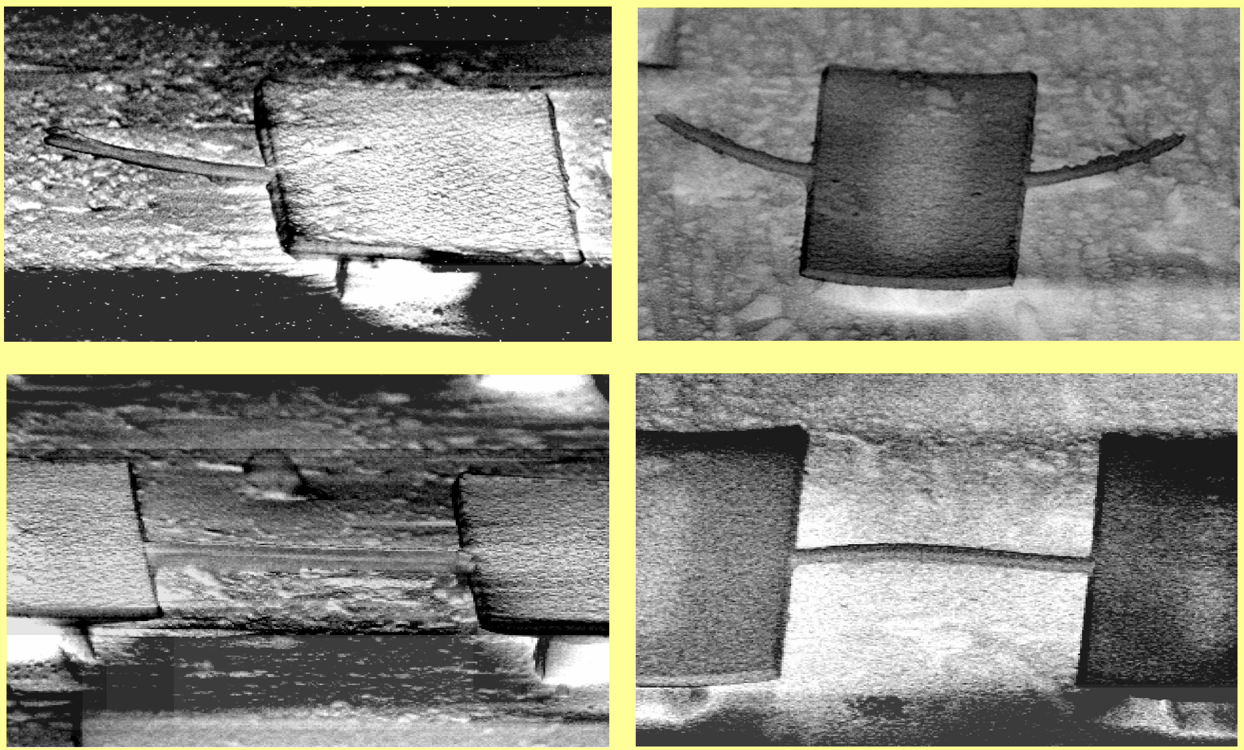

AlN (45 nm)

GaN (120 nm)

} M-plane

γ-LiAlO$_2$(100)

Advantages of AlN
- stiffness
- durability

	Width (mm)	Length (mm)
Cantilevers	0.2	4
Beams	0.2	6

Mismatch	Δa/a (%)	Δc/c (%)
AlN/GaN	2.4	3.9
GaN/γ-LiAlO$_2$	-1.7	-0.3
AlN/γ-LiAlO$_2$	0.7	3.6

Strain relaxation at AlN-GaN interface

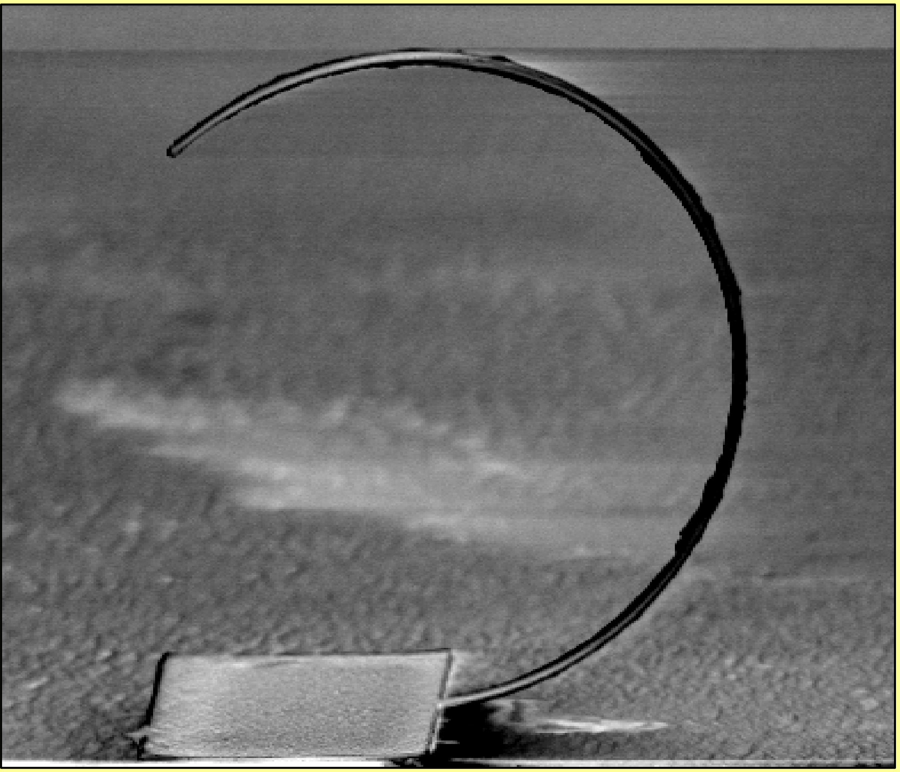

Width 1 mm
AlN thickness 45 nm
GaN thickness 120 nm

Radius of loop 11 mm

Strain estimated from self-rolling

		$[11\bar{2}0]$		[0001]	
d(AlN) (nm)	d(GaN) (nm)	radius (mm)	$\Delta a/a$ (%)	radius (mm)	$\Delta c/c$ (%)
45	120	11	1.0	…	<< 1
70	110	14	0.7	39	0.3
350	515	276	0.2	…	…

Relaxation for thick AlN layers

Almost relaxed along the c axis

Nitrides seem to be good for everything

Dilute Nitrides

(Ga,In)(N,P,As)

cubic

Conventional Nitrides

AlN, GaN, InN

hexagonal (cubic)

Ferromagnetic Nitrides

TE- and RE-doped

hexagonal (cubic)

Bandgap of dilute Nitrides

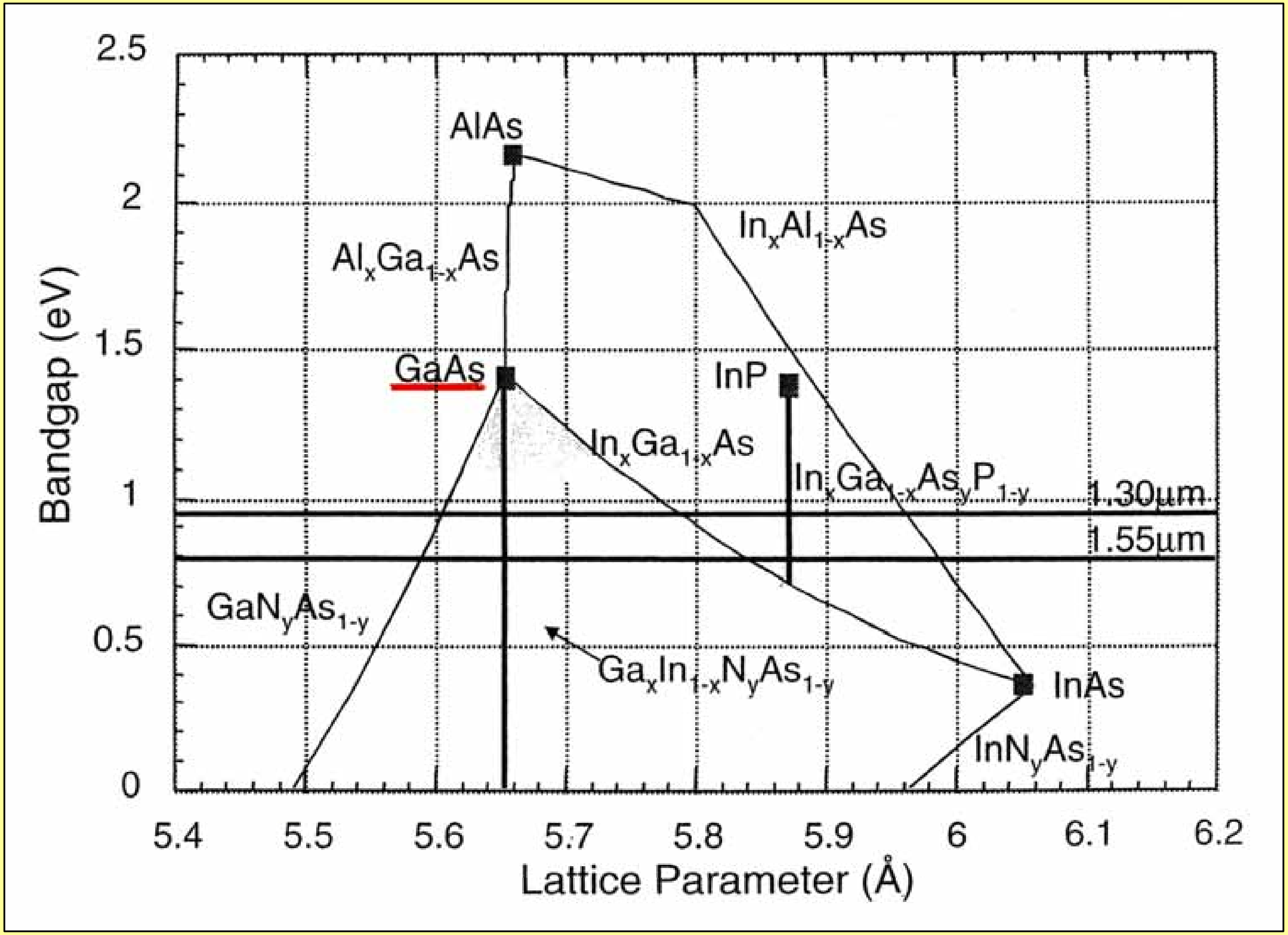

(Ga,In)(N,P,As) alloys lattice-matched to GaAs, GaP or Si (Dilute Nitrides)

- Infrared light emitter
- Multijunction solar cells
- Monolithic integration of Ga(N,P,As)/GaP heterostructure lasers with Si-CMOS circuits („Silicon Photonics")

Problem areas for growth of these metastable alloys

- Large differences in atomic radii and electronegativities of constituent elements
- Large differences in bond strengths of constituent binaries
  - Tendency of alloy clustering enhanced
- Sound models about surface kinetics and growth mechanisms do not exist
  - Empirical optimization of growth conditions
    - Low substrate temperature for 2D growth
    - 2D growth mode stabilized by surfactants?
- Post-growth annealing required to improve internal quantum efficiency
  - Point defects, antisite defects, ion damage ?
  - Deep electron and/or hole traps ?

Major building blocks for Si photonics

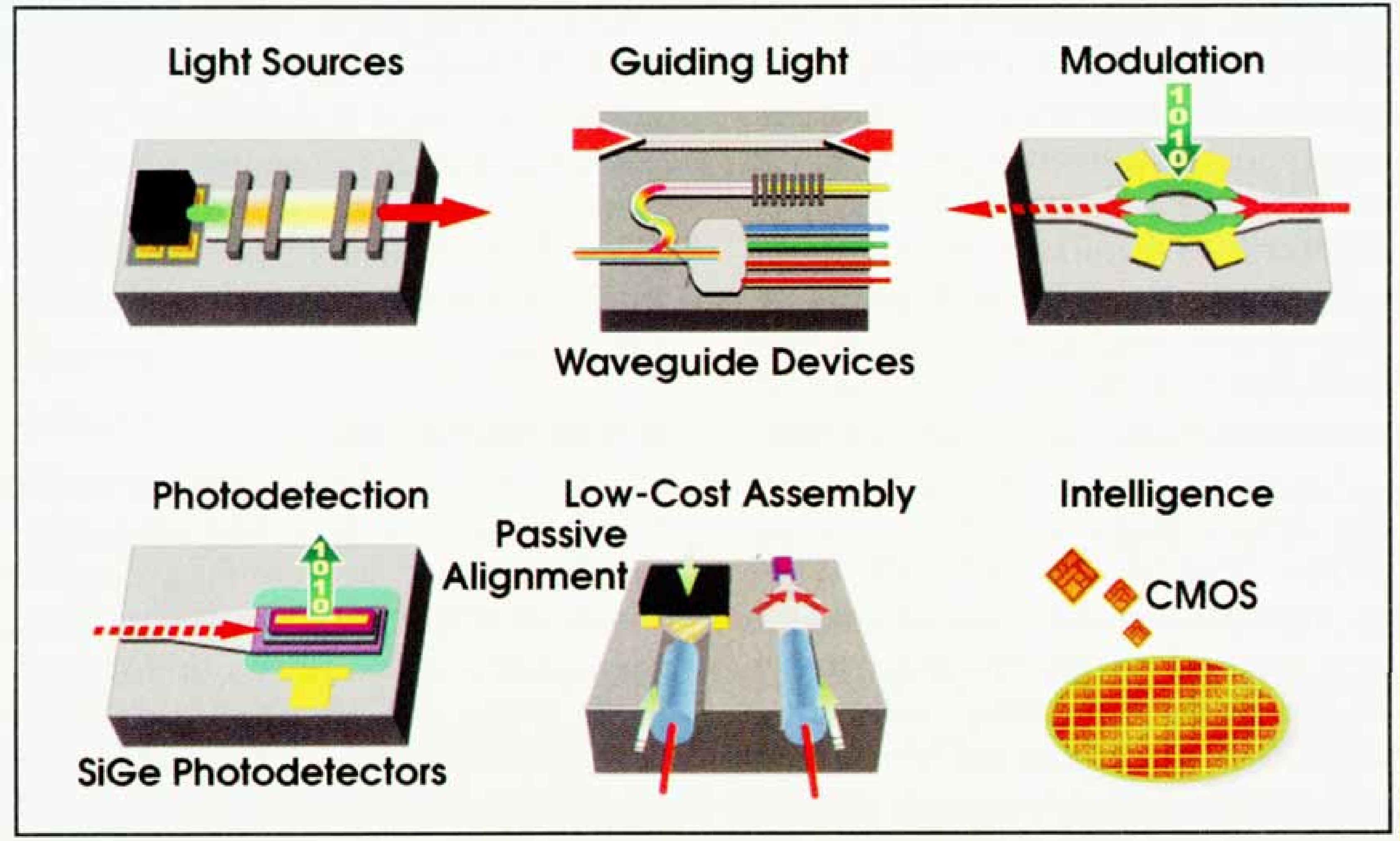

On-chip optical interconnects

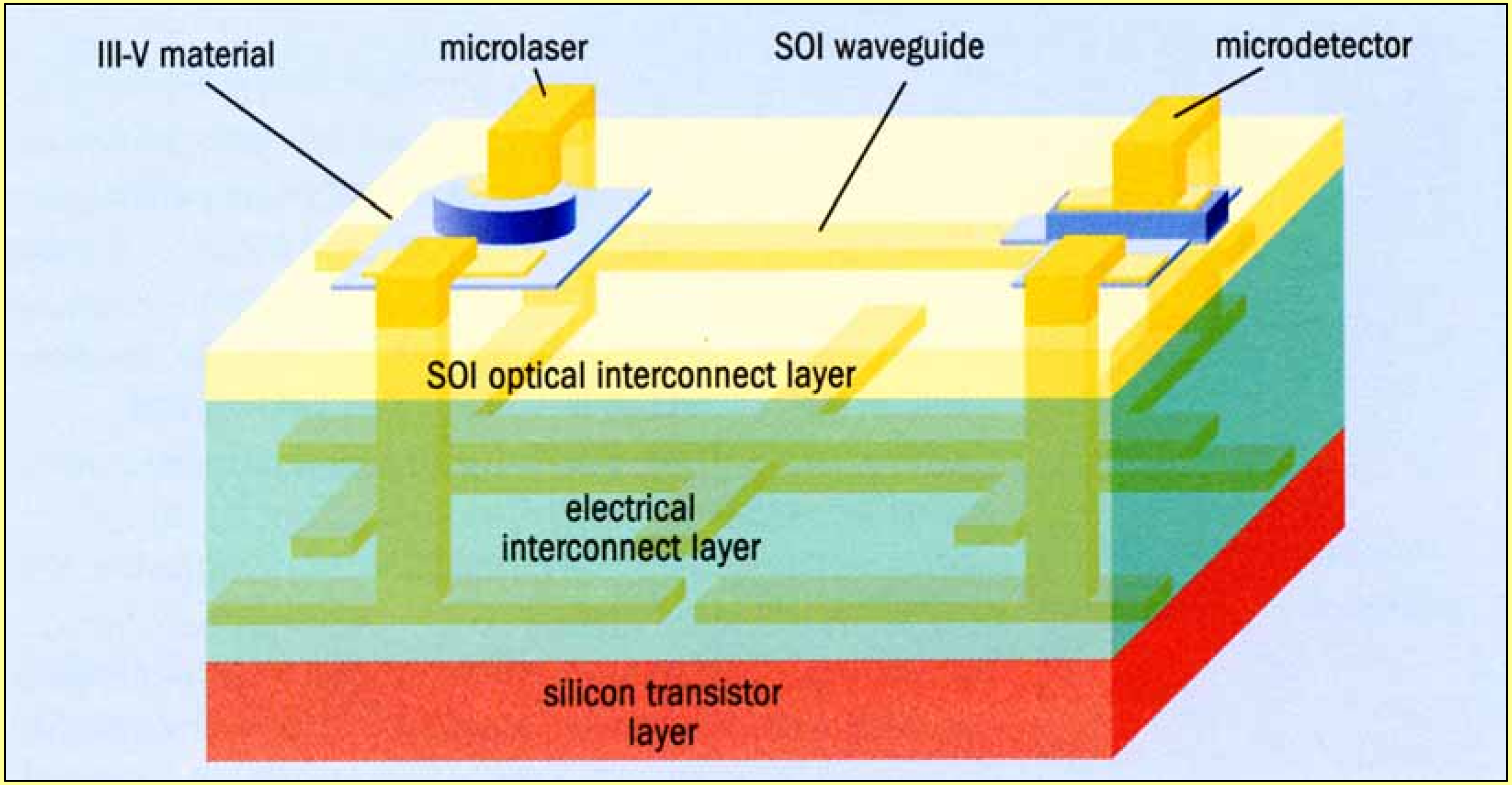

TEM images

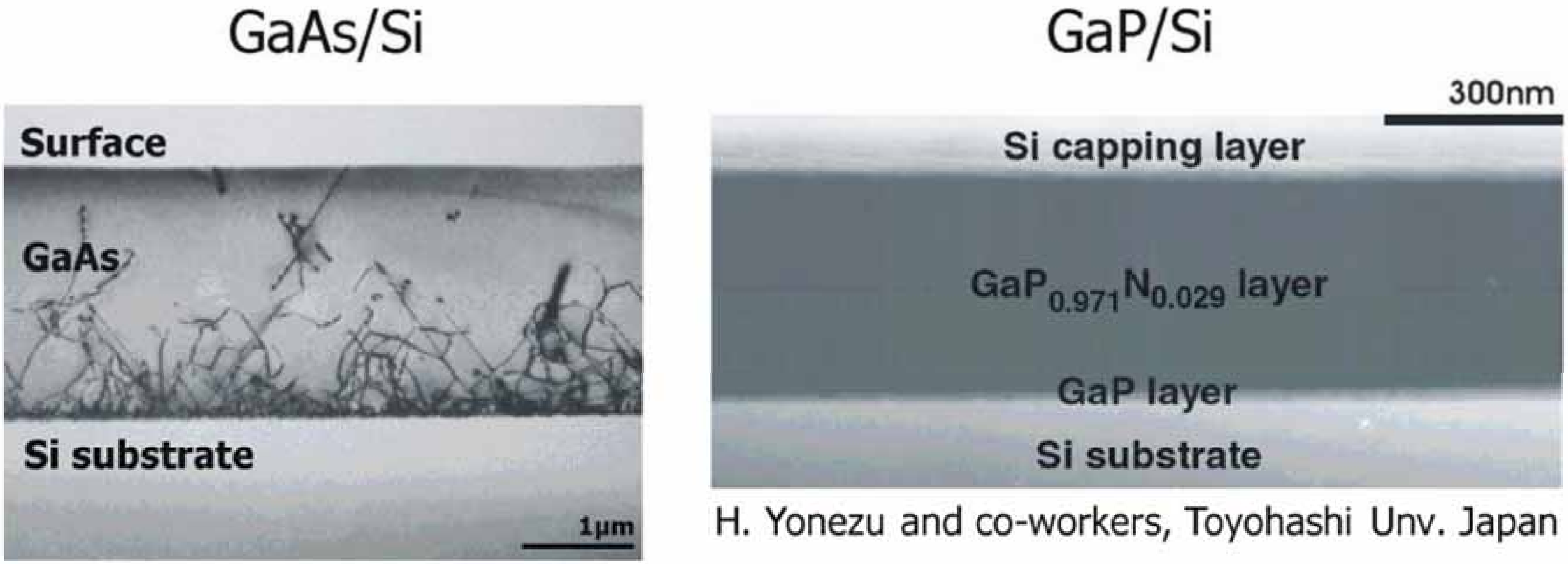

H. Yonezu and co-workers, Toyohashi Unv. Japan

(Ga,In)(N,P,As) alloy

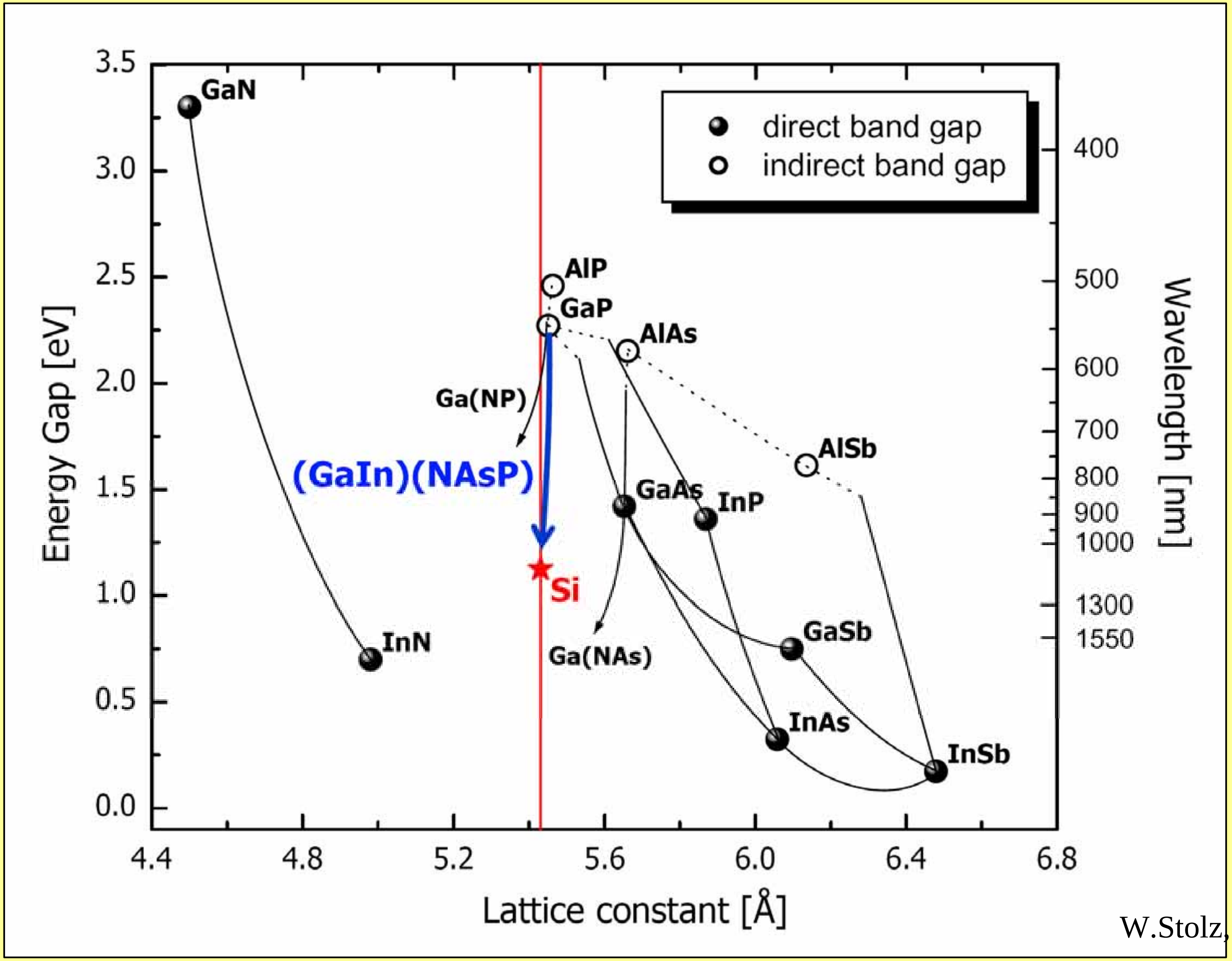

W.Stolz, www.NAsP.de

Proof of concept

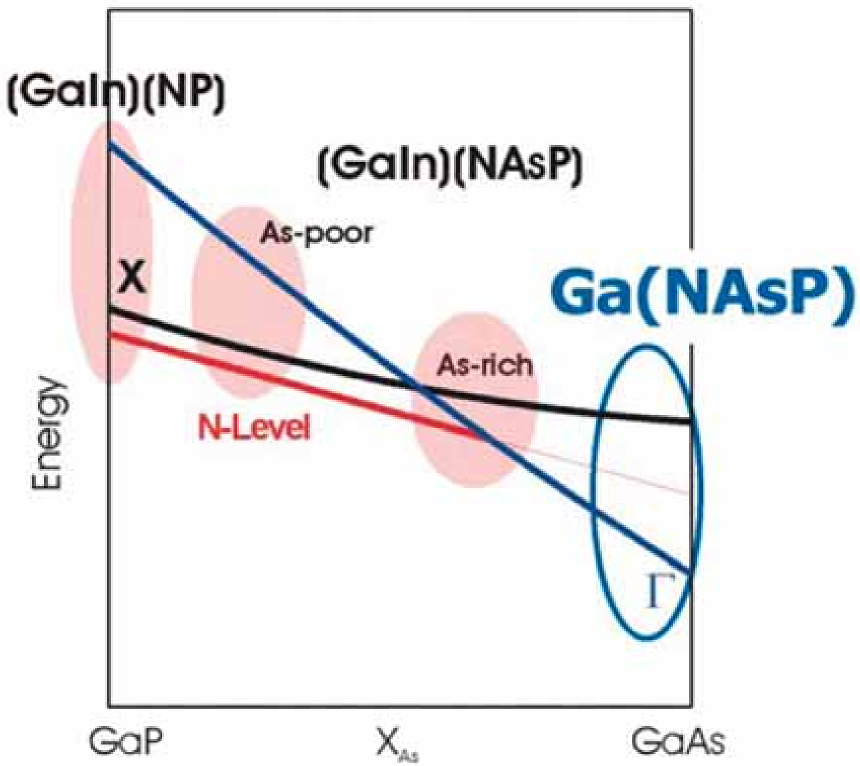

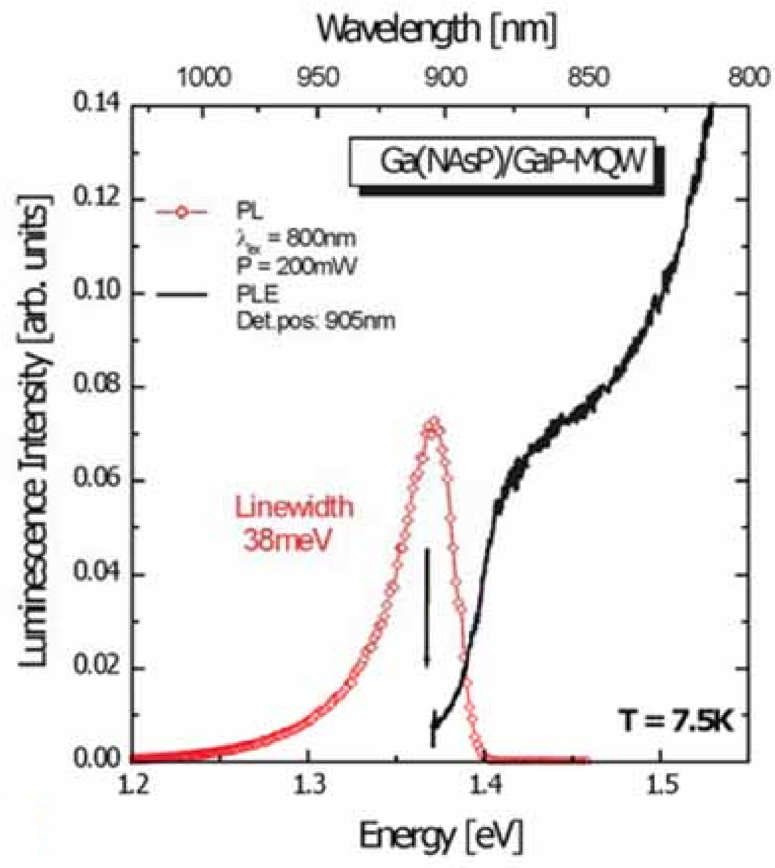

W.Stolz, www.NAsP.de

Estimated vs experimental bandgap

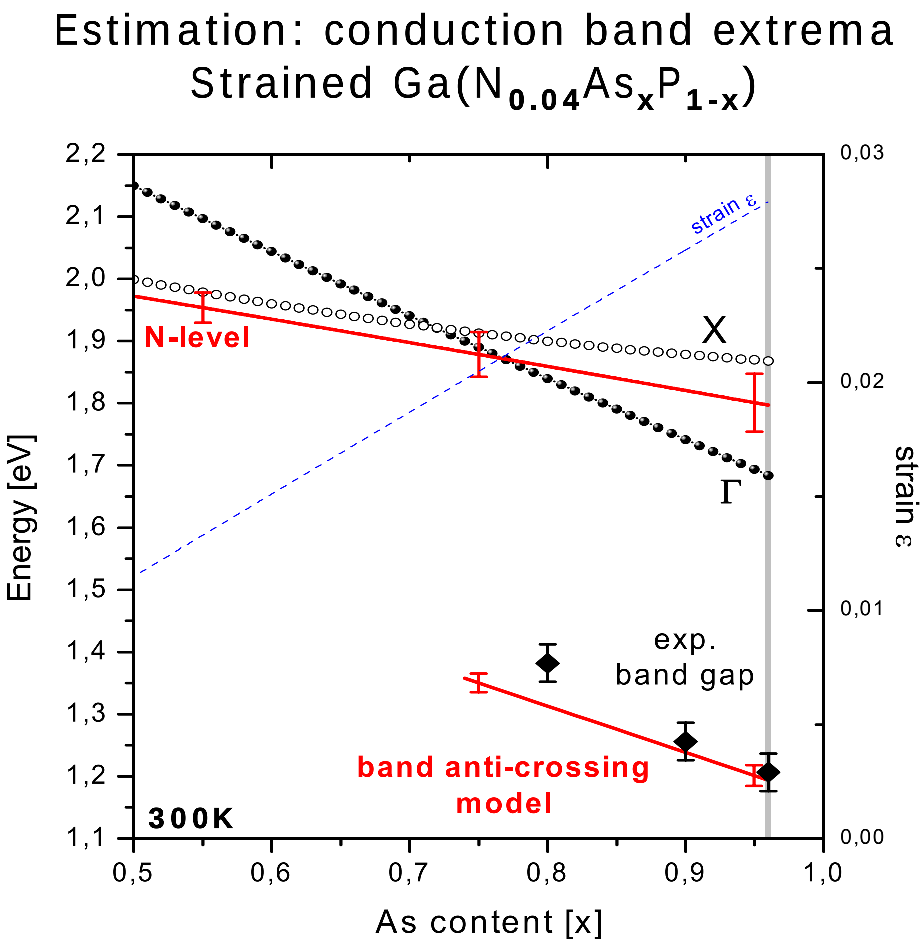

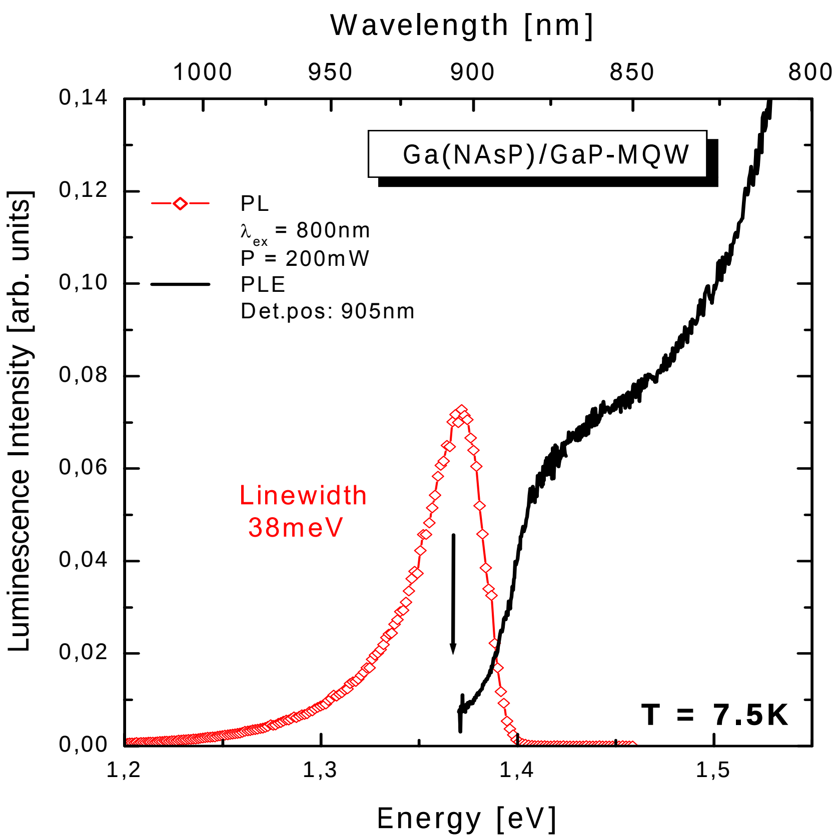

W.Stolz, www.NAsP.de

Band anticrossing (BAC) model

$$E_{-} = \frac{1}{2}\cdot\left[(E_{\Gamma} - \gamma x) + (E_{N} + \alpha x) - \sqrt{((E_{\Gamma} - \gamma x) + (E_{N} + \alpha x))^{2} + 4\cdot\beta^{2} x}\right]$$

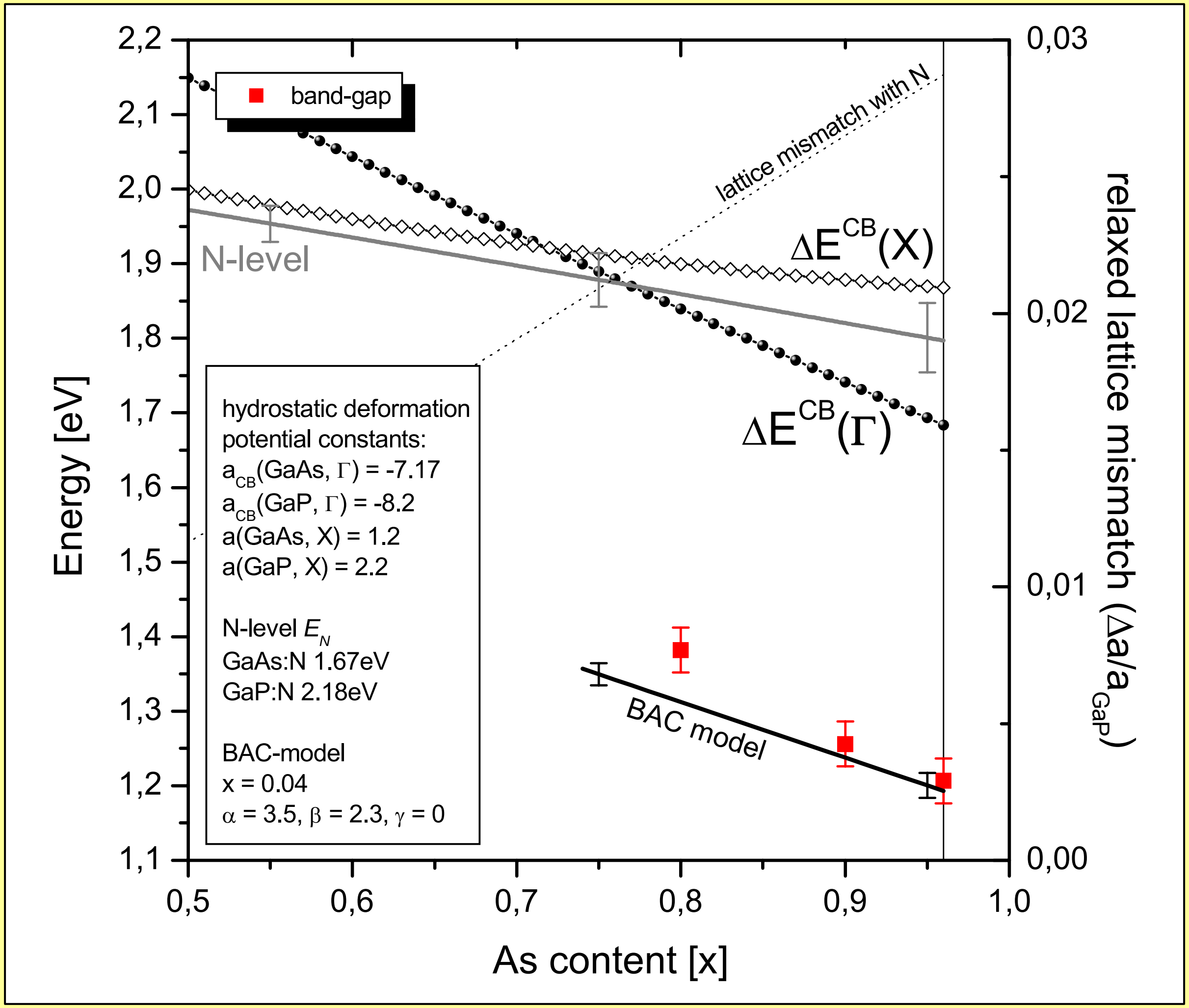

Bandstructure Modification:

Strained $Ga(N_{0.04}As_{x}P_{1-x})$

W.Stolz, www.NAsP.de

Ga(N,P,As) SQW laser

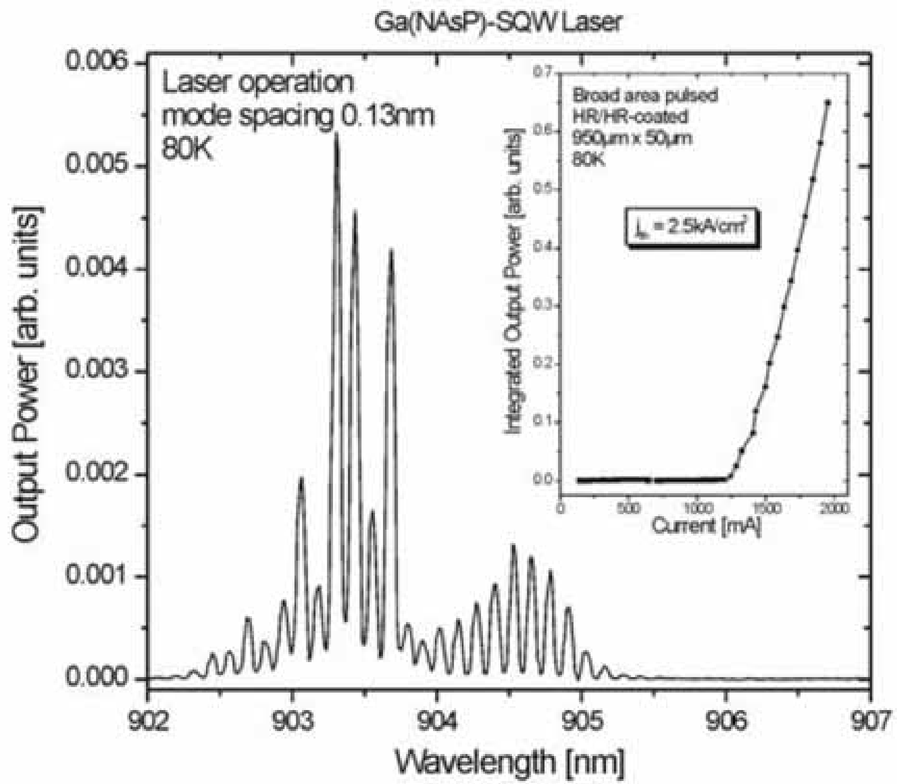

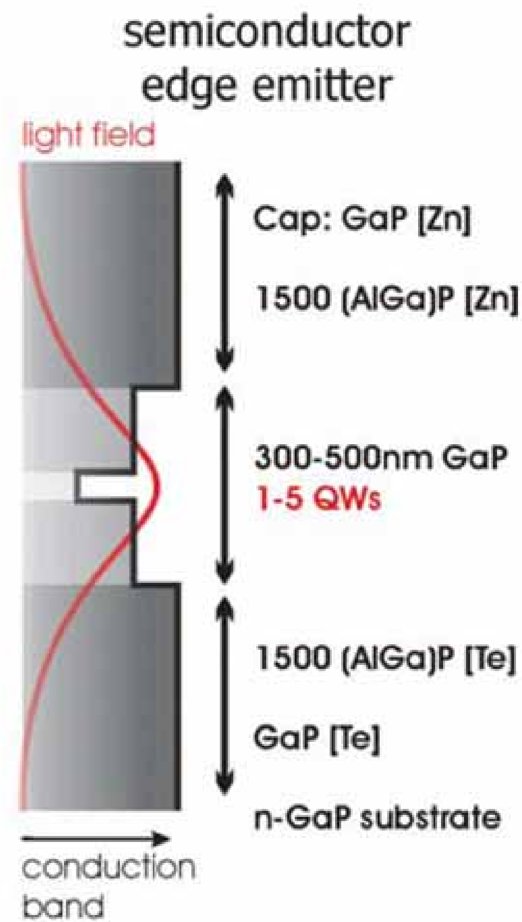

Etched top-p$^+$ contact:
j_{th} = 1.5kA/cm^2

W.Stolz, www.NAsP.de

Nitrides seem to be good for everything

Dilute Nitrides

(Ga,In)(N,P,As)

cubic

Conventional Nitrides

AlN, GaN, InN

hexagonal (cubic)

Ferromagnetic Nitrides

TE- and RE-doped

hexagonal (cubic)

Rare-earth (RE) doping of GaN

- **Sharp RE intra-f-shell optical transitions allow light emission in the visible to infrared spectral range**
  - **Eu-doped GaN → 623 nm emission**
  - **Er-doped GaN → 1.55 µm emission**

- **Isovalent RE^{3+} ions on Ga lattice sites form electrically inert centers (no deep gap states)**

Ref: P. N. Favennec et al., Electron Lett. 25 (1989) 718
Y. Q. Wang and A. J. Steckl, Appl. Phys. Lett. 82 (2003) 402
J. S. Filhol et al., Appl. Phys. Lett. 84 (2004) 2841

- **Magnetic coupling of partially filled 4f-orbitals of RE^{3+} ions possible → weaker than d-orbitals in transition metals**

- **Gd has both partially filled 4f and 5d orbitals → new coupling mechanism?**

Ref: M. Hashimoto et al., Jpn. J. Appl. Phys. 42 (2003) L1112
N. Teraguchi et al., Solid State Commun. 122 (2002) 651

Ferromagnetic nitrides

The mean-field model of free holes mediating ferromagnetism via RKKY interaction have identified wide-gap semiconductors as ideal candidates to generate ferromagnetic semiconductors with high Curie temperature by doping with magnetic transition metal (TM) ions.

Numerous attempts with Mn, Cr, and Fe doping of GaN have yielded inconclusive results.

Doping of GaN with rare earth elements (RE), like Eu, Er, Gd, is well established. Isoelectronic RE species are incorporated on Ga lattice sites.

Gd concentration vs Gd/Ga flux ratio

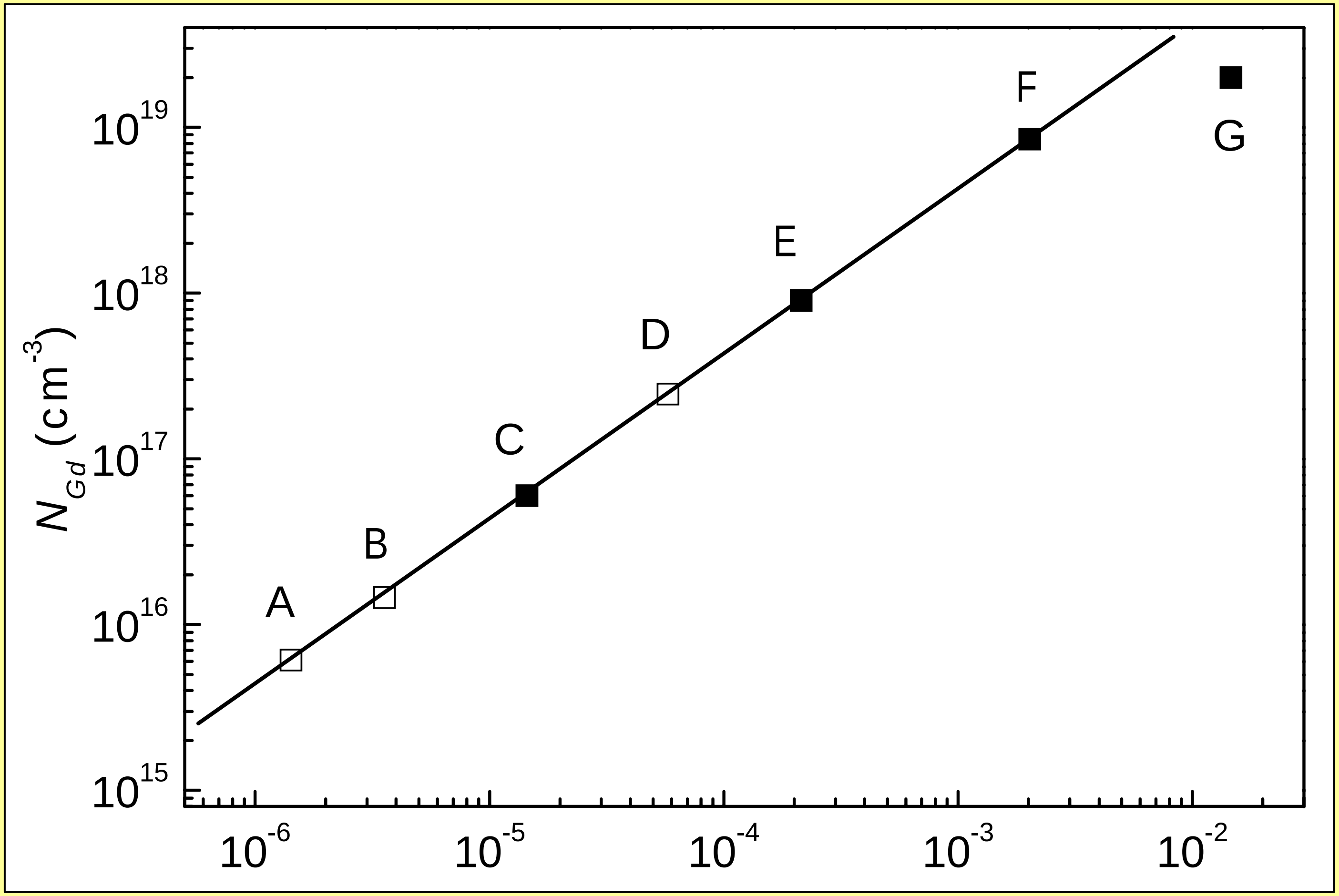

Unity sticking coefficient of Gd up to 10^{19} cm^{-3}

Magnetic hysteresis ([Gd] = 6 x 10^{16} cm^{-3})

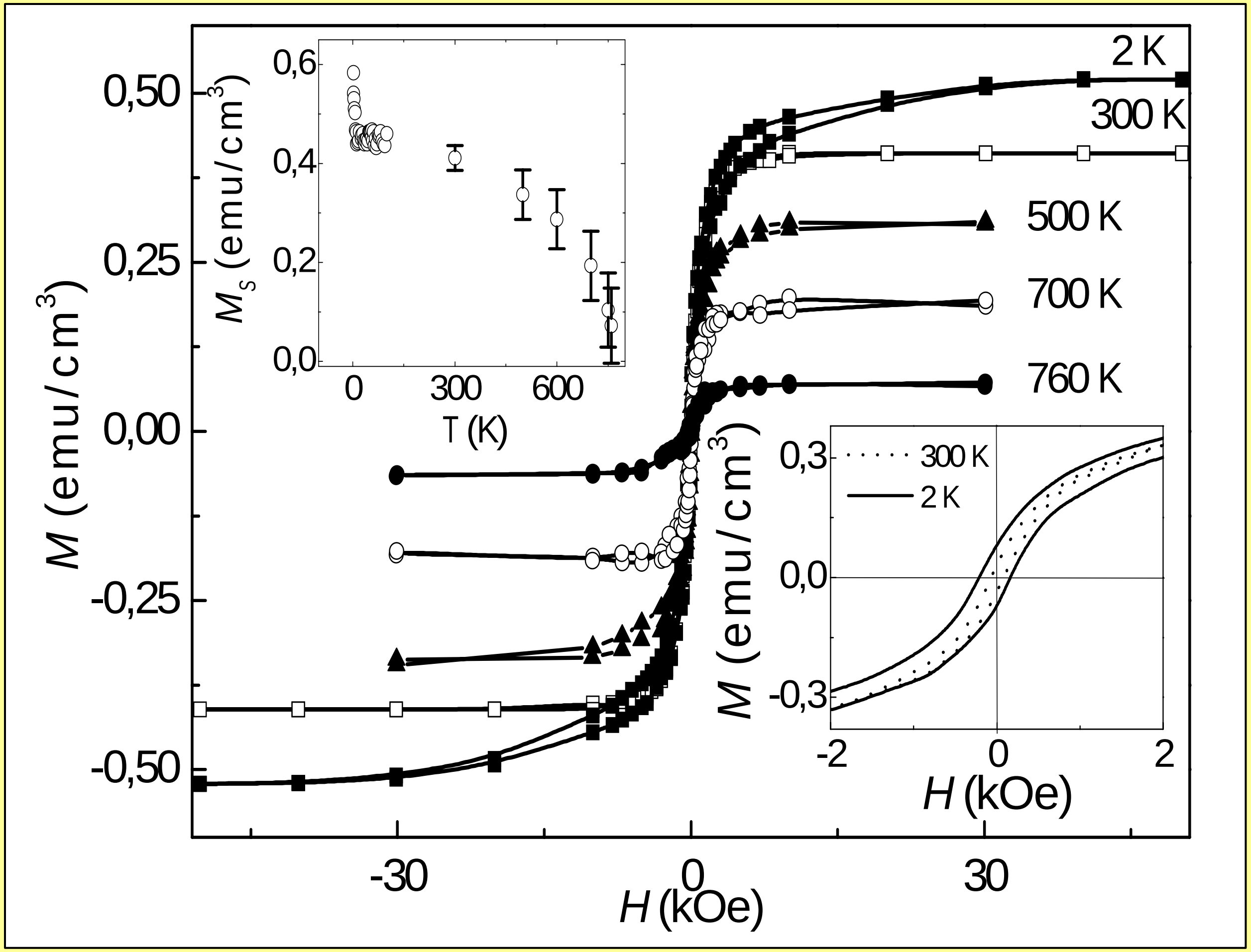

- Magnetization saturates at high fields $\Rightarrow$ Ferromagnetism
- Superposition of two loops with different H_c and M_r at 2 K ?
  $\rightarrow$ above 10 K phase with larger H_c and M_r disappears

Saturation magnetization vs [Gd]

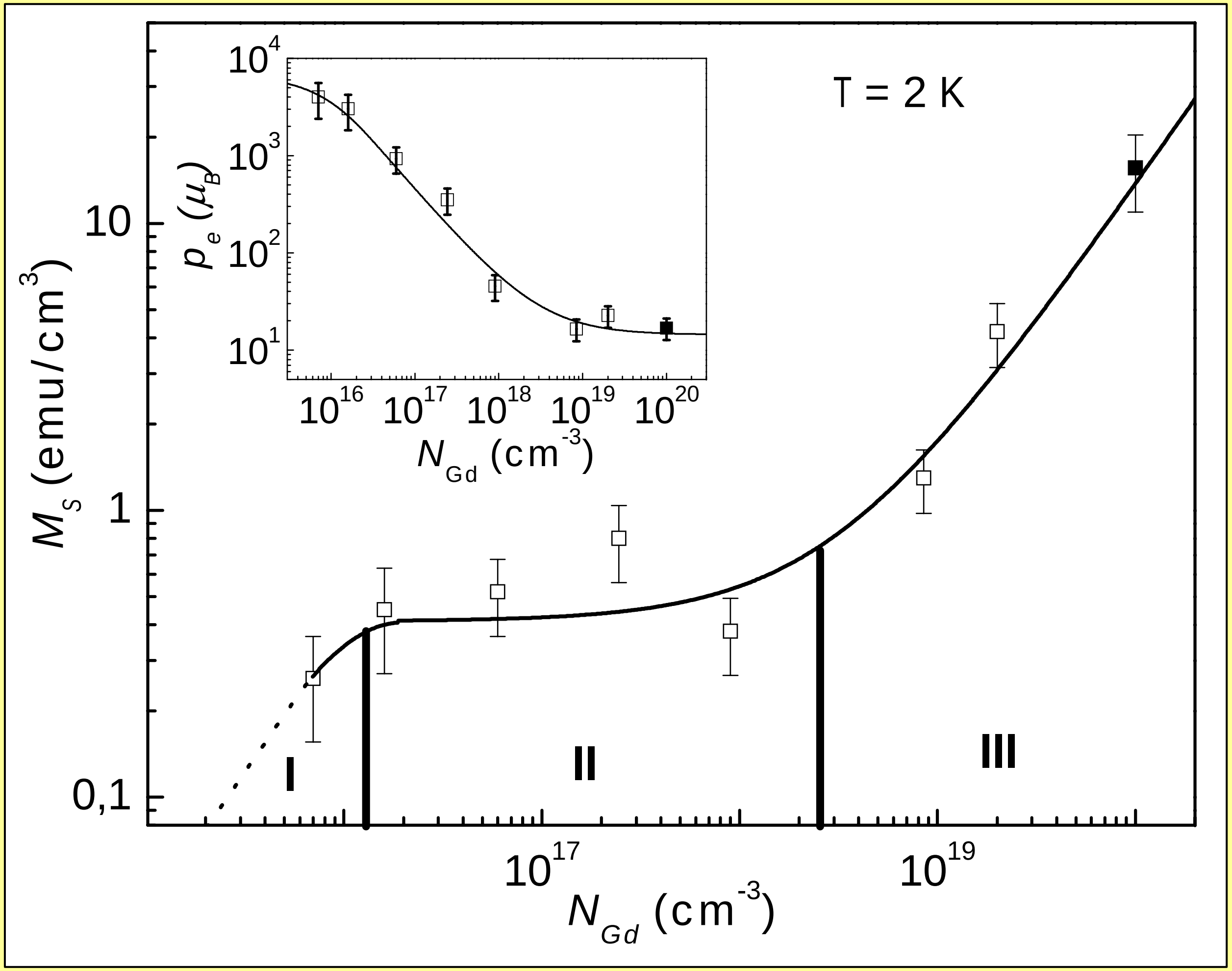

Inset: Magnetic moment per Gd atom

Empirical model for origins of colossal moment

Gd atoms polarize the matrix

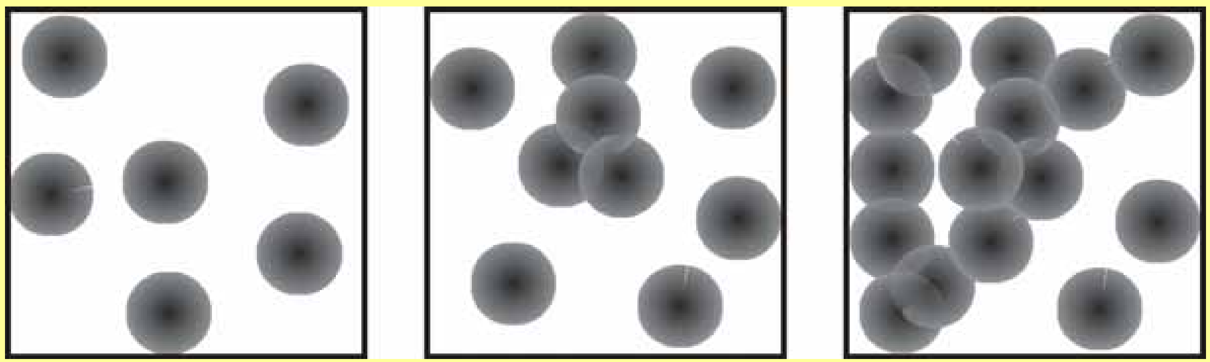

$$p_e = p_{Gd} + p_m\, \nu\, N_o/N_{Gd};\ \nu = 1\text{-exp}(-v\, N_{Gd})$$

p_e decreases as N_{Gd} is increased $\rightarrow$ experimentally observed

Overlap of spheres $\rightarrow$ ferromagnetic coupling

T_c increases with N_{Gd} $\rightarrow$ experimentally observed

Magnetization curves of Gd-doped GaN measured in two perpendicular directions

6 x 10^{16} cm^{-3}

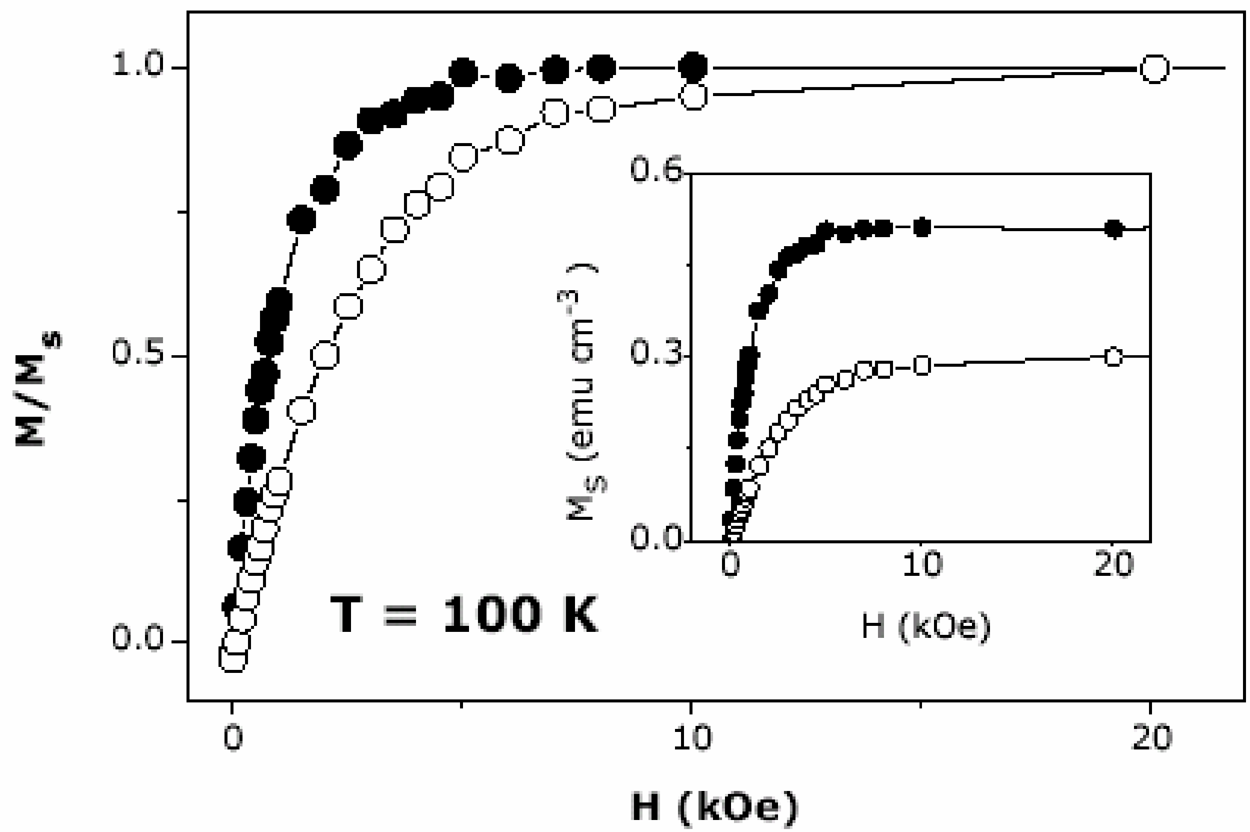

Saturation magnetization is smaller along hard axis

Magnetic moment of Gd in implanted GaN

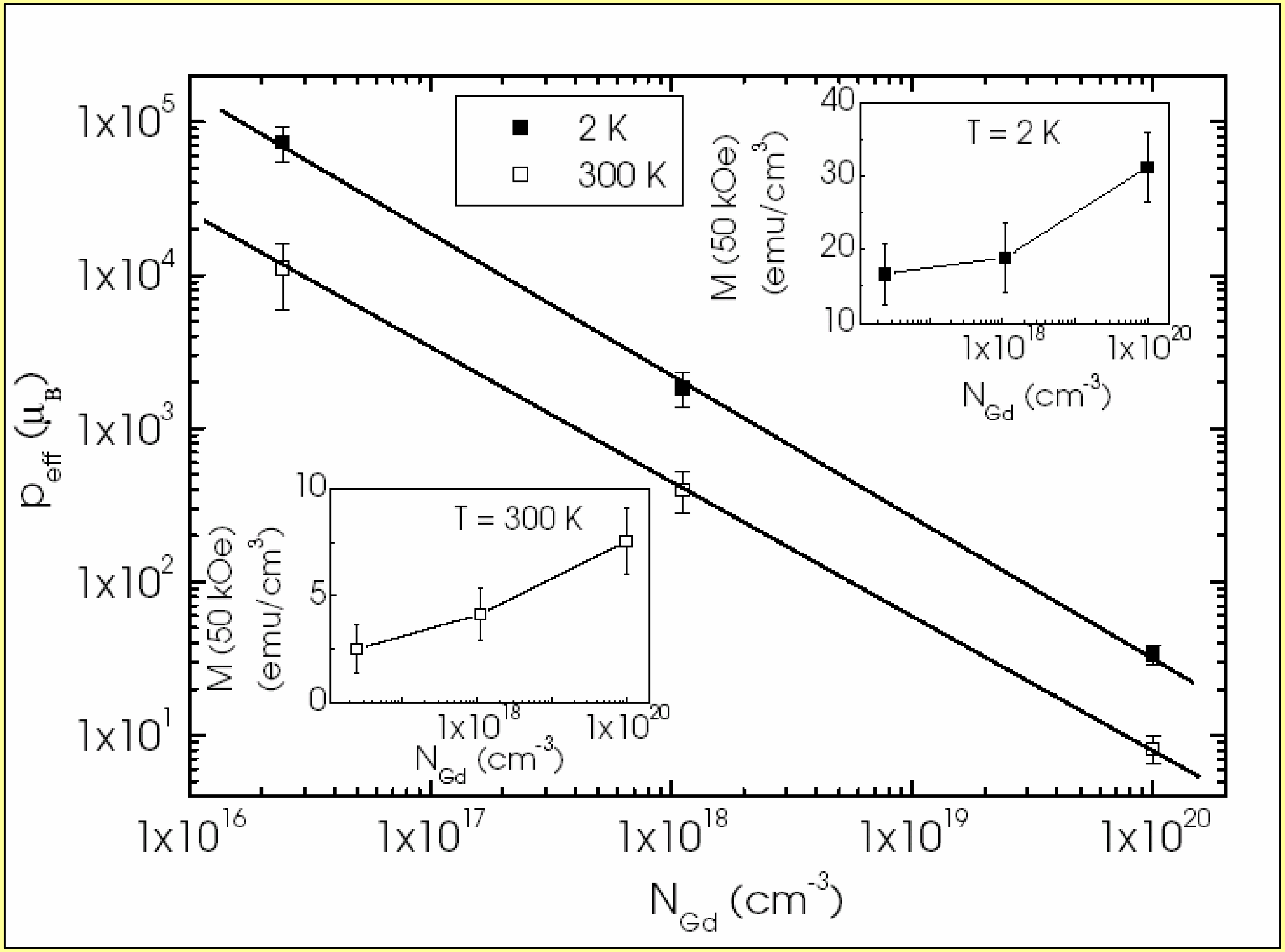

Saturation magnetization shown in insets

FC and ZFC magnetization in Gd-implanted GaN

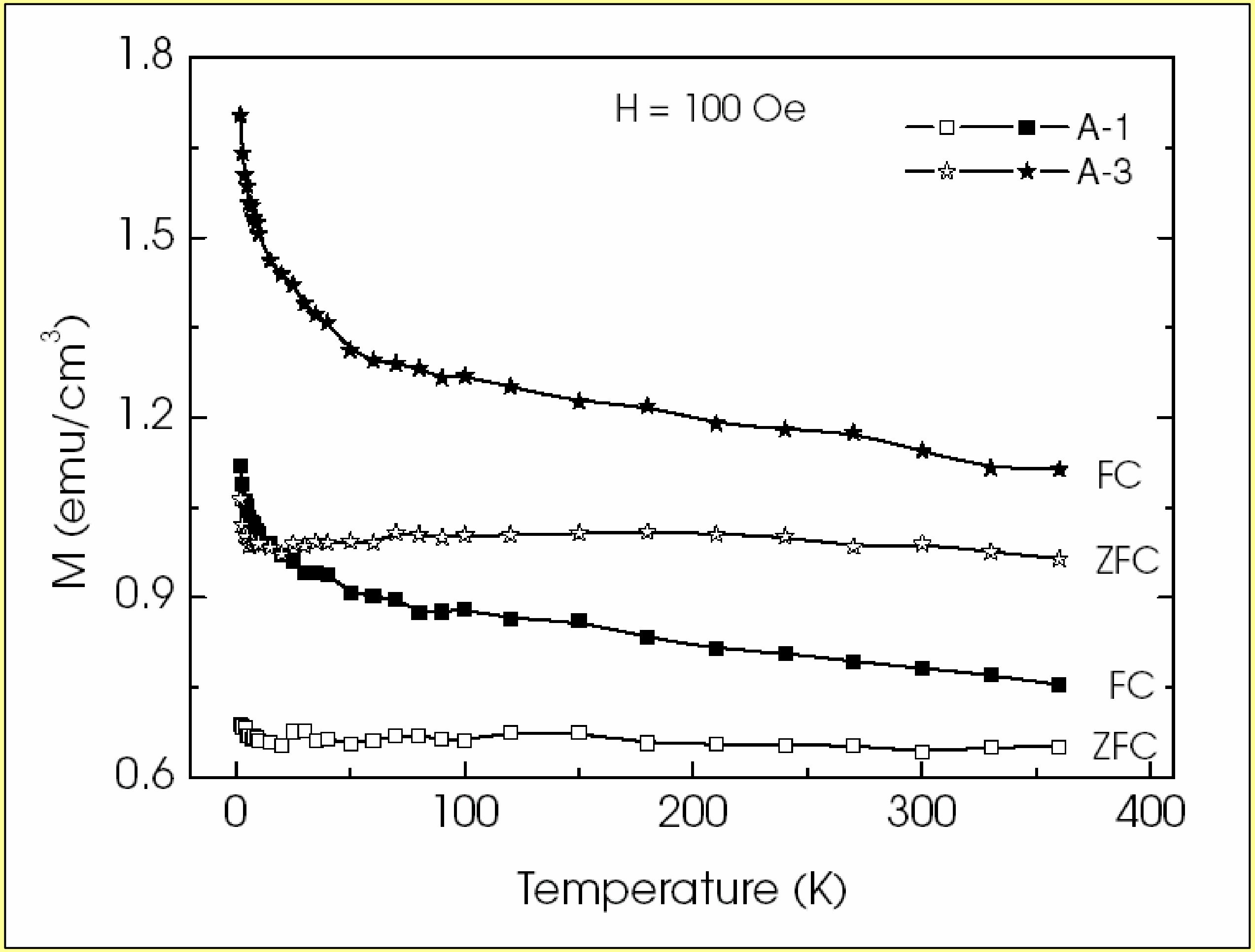

A-1 2 x 10^{16} cm^{-3}

A-3 1 x 10^{20} cm^{-3}

Magnetic hysteresis of Gd-implanted GaN

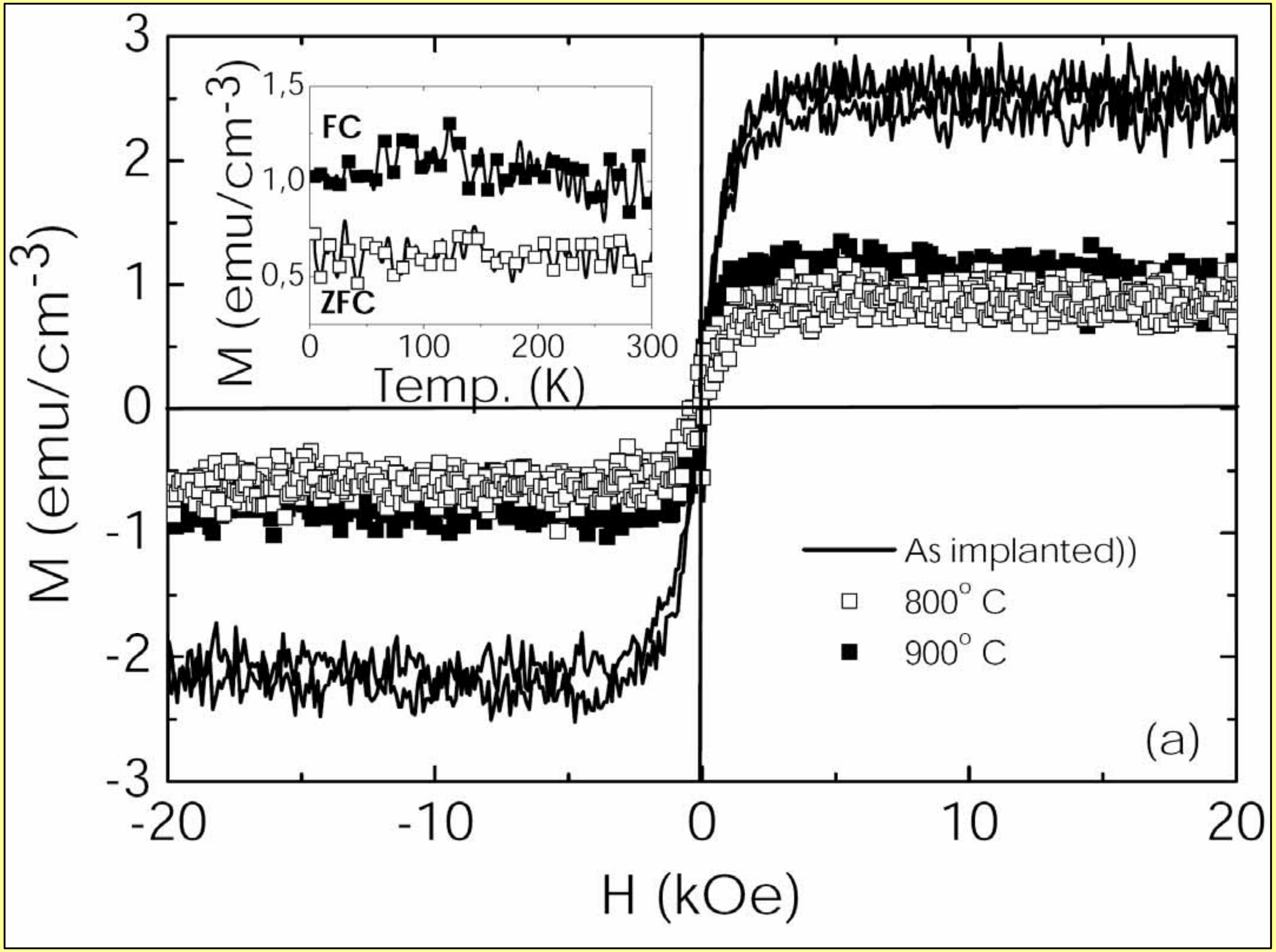

S.Dhar et al., APL 91(2007)072514

Results from Gd-doped GaN

Single-phase Gd-doped GaN layers show ferromagnetic behavior with in-plane easy axis and high Tc

Colossal magnetic moment per Gd atom

Coexistence of two ferromagnetic phases with different order temperatures

Measured saturation magnetization depends on orientation of the magnetic field

Structural defects play important role for magnitude of colossal magnetic moment per Gd atom

Empirical model based on polarization of entire GaN matrix by Gd dopants (an/or defects) can explain the observed colossal magnetic moment

Role of defects in creating ferromagnetism in semiconductors (polaron model)

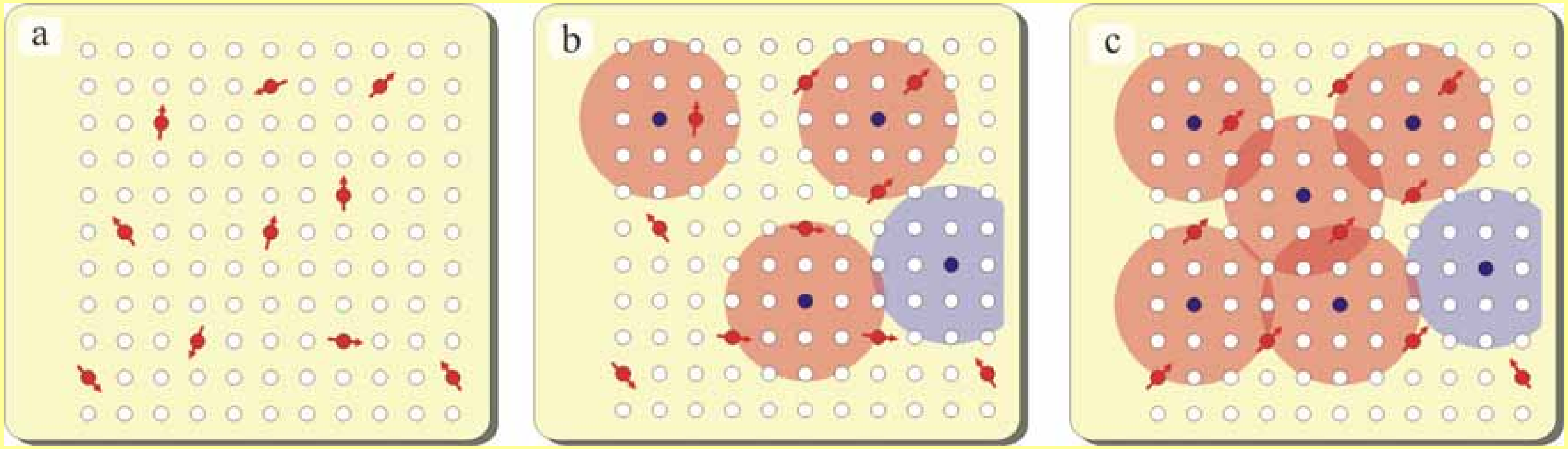

J.M.D. Coey et al., Nature Mater. 4(2005)173

III-Nitride nanostructures

Large number and wide variety of nano-objects consisting of III-Nitrides, including

- quantum wires
- nanowires
- nanocolumns
- nanorodes
- quantum dots
- nanodots
- etc

have been fabricated by different growth techniques.

Challenges are to have control over

- size (geometrical dimensions)
- uniformity
- placements
- interconnects (for electrnic access)

Concluding remarks

issues & events

US condensed-matter community grapples with availability of crystalline samples

Crystal growing for physics measurements has fallen between the cracks in the US; without a turnaround, the country can't help but lag in the discovery of new materials and their applications.

Physics Today, August 2007, p.26